Molecular Phylogenetics and Evolution 190 (2024) 107944

Contents lists available at ScienceDirect

Molecular Phylogenetics and Evolution

journal homepage: www.elsevier.com/locate/ympev

Paraphyly and cryptic diversity unveils unexpected challenges in the "naked lichens" (*Calvitimela*, Lecanoromycetes, Ascomycota)

Markus Osaland Fjelde [a,b,*], Einar Timdal [a], Reidar Haugan [a], Mika Bendiksby [a,c]

[a] Natural History Museum, University of Oslo, P.O. Box 1172 Blindern, NO-0318 Oslo, Norway
[b] Section for Genetics and Evolutionary Biology, Department of Biosciences, University of Oslo, P.O. Box 1066 Blindern, NO-0316, Norway
[c] NTNU University Museum, Norwegian University of Science and Technology, 7491 Trondheim, Norway

ARTICLE INFO

Keywords:
Cryptic species
Integrative taxonomy
Lichenized fungi
Phylogenetics
Substitutional saturation
Secondary chemistry

ABSTRACT

Molecular phylogenetics has revolutionized the taxonomy of crustose lichens and revealed an extensive amount of cryptic diversity. Resolving the relationships between genera in the crustose lichen family Tephromelataceae has proven difficult and the taxon limits within the genus *Calvitimela* are only partly understood. In this study, we tested the monophyly of *Calvitimela* and investigated phylogenetic relationships at different taxonomic levels using an integrative taxonomic approach. We performed a global sampling of all species currently assigned to *Calvitimela* and conducted additional sampling of *C. melaleuca* sensu lato across Norway. We included 108 specimens and produced more than 300 sequences from five different loci (ITS, LSU, MCM7, mtSSU, TEF1-α). We inferred phylogenetic relationships and estimated divergence times in *Calvitimela*. Moreover, we analyzed chemical and morphological characters to test their diagnostic values in the genus. Our molecular phylogenetic results show evolutionarily old and deeply divergent lineages in *Calvitimela*. The morphological characters are overlapping between divergent subgenera within this genus. Chemical characters, however, are largely informative at the level of subgenera, but are often homoplastic at the species level. The subgenus *Calvitimela* is found to include four distinct genetic lineages. Detailed morphological examinations of *C. melaleuca* s. lat. reveal differences between taxa previously assumed to be morphologically cryptic. Furthermore, young evolutionary ages and signs of gene tree discordance indicate a recent divergence and possibly incomplete lineage sorting in the subgenus *Calvitimela*. Phylogenetic analysis and morphological observations revealed that *C. austrochilensis* and *C. uniseptata* are extraneous to *Calvitimela* (Tephromelataceae). We also found molecular evidence supporting *C. septentrionalis* being sister to *C. cuprea*. In the subgenus *Severidea*, one new grouping is recovered as a highly supported sister to *C. aglaea*. Lastly, two fertile specimens were found to be phylogenetically nested within the sorediate species *C. cuprea*. We discuss the need for an updated classification of *Calvitimela* and the evolution of cryptic species. Through generic circumscription and species delimitation we propose a practical taxonomy of *Calvitimela*.

1. Introduction

Lichenized fungi represent one of the most common ecological modes in the fungal kingdom. Lichens are a symbiosis between one fungal (the mycobiont) and one green algal and/or cyanobacterial (the photobiont) component (Nash, 2008). The idea that lichens are symbiotic partnerships has been around since the late 1800s (Schwendener, 1869). Recently, a large body of work highlighted the importance of additional symbionts (i.e., other fungi and bacteria; e.g., Cardinale et al., 2006; Arnold et al., 2009; Hodkinson and Lutzoni, 2009; Spribille et al., 2016). Nevertheless, the taxonomy of lichens is based on the main mycobiont (i.e., the fungus with the greatest cellular abundance), which usually is the ascomycete fungus forming the lichen thallus.

The regular toolbox to identify lichens includes a hand lens and some bottles of chemical compounds for species identification in the field (e.g., Stenroos et al., 2016), and a microscope for anatomical investigations and species determination keys for inhouse determination work (e.g., McCune, 2017; Purvis et al., 1992). Additionally, thin-layer chromatography (TLC), which is a technique that has been used for over half a century (e.g., Culberson & Kristinsson, 1970; Culberson & Johnson,

* Corresponding author at: Section for Genetics and Evolutionary Biology, Department of Biosciences, University of Oslo, P.O. Box 1066 Blindern, NO-0316 Oslo, Norway.
E-mail address: markusof@uio.no (M.O. Fjelde).

https://doi.org/10.1016/j.ympev.2023.107944
Received 29 December 2021; Received in revised form 28 September 2023; Accepted 13 October 2023
Available online 14 October 2023

1982; Haugan & Timdal, 1994; Spribille et al., 2011b) can be used to distinguish species based on their chemical profile of lichen acids (hereafter referred to as "chemistry"). During the last three decades, DNA sequencing technology has become an increasingly important tool for both species' identification (DNA barcoding; e.g., Kelly et al., 2011; Marthinsen et al., 2019) and species delimitation (e.g., Leavitt et al., 2011; Singh et al., 2015a). Whereas many lichens are identifiable by the naked eye, others require microscopy or TLC. Among crustose lichens (lichens which grow tightly attached to their substrates), a third group of phenotypically cryptic species are frequent and require DNA sequences data for identification (see Zhang et al., 2022).

The traditional way of circumscribing lichen species based on morphological and chemical traits is still central to lichen taxonomy. Crustose lichens have few morphological characters, and for this reason TLC has been essential for species recognition and delimitation. However, not all lichens have detectable or informative chemistry (see LaGreca et al., 2020). Even when including all available morphological and TLC data, the combination may not be enough to reach sensible species hypotheses. One recommended way to circumscribe fungal species is through an integrative approach combining phenotypic, genotypic, and geographic data (Lücking et al., 2020). The process usually starts with species hypotheses as monophyletic groups in a molecular phylogeny, using a genealogical concordance approach (Taylor et al., 2000) if multiple genes are available. The idea behind the integrative approach is that data from various sources of evidence can be used to test if the initial hypothesis is supported and thus provide a more robust framework for recognizing species.

A large number of cryptic species has been revealed using molecular phylogenetics (e.g., Crespo and Lumbsch, 2010; Bendiksby et al., 2013; Singh et al., 2015a; Schneider et al., 2016; Leavitt et al., 2016). Following the discovery of cryptic species, however, diagnostic morphological traits can become evident (e.g., Frolov et al., 2016). Such species are often referred to as semi- or pseudocryptic (e.g., Mann & Evans, 2008). Two related concepts in lichenology are the terms "species pair" and "sibling species". The former refers to the phenomenon when two lichens differ only by their reproductive strategies (see Poelt, 1970; Mattson & Lumbsch, 1989), where a "primary species" produces sexual reproductive structures and a "secondary species" reproduce by asexual propagules or fragmentation. The latter refers to a special case of cryptic species: "…Species recognized primarily by cryptic or non-morphological discontinuities" (Culberson, 1986), essentially meaning morphologically indistinguishable taxa with, for instance, different chemistries. Today, a more restricted definition of sibling species refers to cryptic species that are monophyletic (Lumbsch and Leavitt, 2011). The term "chemosyndrome" has been used to explain the phenomenon when different sets of biogenetically related substances are produced by distinct species of lichens (Culberson & Culberson, 1976). This concept is useful for classifying more complex patterns of chemical variation in lichens.

In addition to establishing species hypotheses and identifying species, inferring the evolutionary history based on DNA sequence data is useful for understanding the processes by which organisms and their attributes change through time (e.g., Nelsen et al., 2020). Such processes may include both extrinsic selective forces as well as intrinsic mechanisms (e.g., Gaya et al., 2015), some of which may contribute to a more holistic understanding of the study group, which could lead to a taxonomical revision. Molecular phylogenies can provide unique insight into changes in character composition and how they contribute to evolutionary innovations (see Huang et al., 2019) or shed light on reproductive barriers (Keuler et al., 2022). Also, it can help understanding biogeographical patterns (Garrido-Benavent et al., 2021) and identifying factors involved in trophic transitions (Arnold et al., 2009). This makes it a "prime tool" for understanding the main drivers of biodiversity, namely speciation. Only through the lens of evolutionary biology and how it relates to a specific snapshot of contemporary diversity can we settle on a consistent and natural classification of taxa.

A common practice in molecular systematics has been to use a few informative loci (Lutzoni et al., 2004). However, this can be associated with difficulties in resolving deeper divergences. It has been shown that in some cases, very large data sets (high number of loci and taxa) are needed to render supported backbone resolution (e.g., Pizarro et al., 2018). Other times, when speciation occurred over short time intervals (i.e., rapid radiations), adding more data will not necessarily solve the problem (Philippe et al., 2011; Lemmon & Lemmon, 2013; Widhelm et al., 2019; Pardo-De la Hoz et al., 2023). In some lichen groups, the inability to resolve deep phylogenetic relationships is a major set-back for circumscription of natural taxa (e.g., Bendiksby et al., 2015). Understanding what may cause the resolution to vary within and across genetic markers is invaluable knowledge in molecular systematics.

The lichen genus *Calvitimela* Hafellner ("the naked lichens") represents an example of a clade with poor phylogenetic backbone resolution (Fig. 1A; Fig. 2 of Bendiksby et al., 2015). This is a circumpolar lichen genus that together with the genera *Mycoblastus* Norman, *Tephromela* M. Choisy, and *Violella* T. Sprib. form the family Tephromelataceae (Lecanorales, Lecanoromycetes). In the most recent update on ascomycete taxonomy, Lücking et al. (2017) indicated that there are approximately 10 species of *Calvitimela*, 10 of *Mycoblastus*, 30 of *Tephromela*, and two of *Violella*. These are crustose lichens inhabiting rocks and plants in primarily alpine, arctic, and boreal regions. Although these four genera constitute a well-supported monophyletic family, the Tephromelataceae, their interrelationships remain unresolved (e.g., Spribille et al., 2011a; Bendiksby et al., 2015). Two of the species in *Calvitimela*, from the Southern Hemisphere (*C. austrochilensis* Fryday, *C. uniseptata* G. Thor), represent poorly understood members of the genus.

In their molecular phylogenetic study of *Calvitimela* sensu lato (=subgenera *Calomela*, *Calvitimela*, *Paramela*, *Severidea*), based on three nuclear markers (ITS, TEF1-α, MCM7), Bendiksby et al. (2015) pointed to two main challenges at different taxonomic levels. These include: (1) The largely unresolved phylogenetic relationships between the genera *Tephromela* and *Violella* and the four subgenera of *Calvitimela* (i.e., *Calomela*, *Calvitimela*, *Paramela*, and *Severidea*); and (2) The taxonomic challenges of subgen. *Calvitimela* (i.e., *Calvitimela* sensu stricto), which includes a paraphyletic *C. melaleuca* (Fig. 1A), uninformative morphology, and a confusing pattern of secondary metabolites.

In this study, we present the first part of a two-part project where we use an integrative taxonomic approach to reach a better understanding of *Calvitimela*. Specifically, we address the two challenges stated above. We combine molecular phylogenetics with studies of morphology and chemistry to study *Calvitimela* from the level of genus circumscription, through species delimitation and phylogenetic interrelationships, to population structure in *C. melaleuca*. The study is based on a broad and global taxon sampling of all available species, and a denser sampling of *C. melaleuca* s. lat. from Norway. Much effort has been put into identifying phylogenetically informative morphological and chemical characters, including in-depth investigations of cryptic species. Lastly, we explore the sources of non-phylogenetic signals in the molecular data and assess the genetic markers' abilities to resolve phylogenetic relationships at different taxonomic levels.

2. Material and methods

2.1. Taxon sampling

We have investigated specimens of all currently recognized *Calvitimela* species including the two poorly understood Southern Hemisphere species *C. austrochilensis* and *C. uniseptata*. We have included 67 freshly collected specimens, collected in Norway during the summers of 2019 and 2020, and 87 specimens from throughout the global distribution of the genus, deposited in different fungaria (i.e., GZU, KGLO, MSC, O, QFA, UPS, and WIS; Table S1).

We collected samples using hammer and chisel and dried them in paper bags before they were brought to Fungarium O (NHM, UiO) for

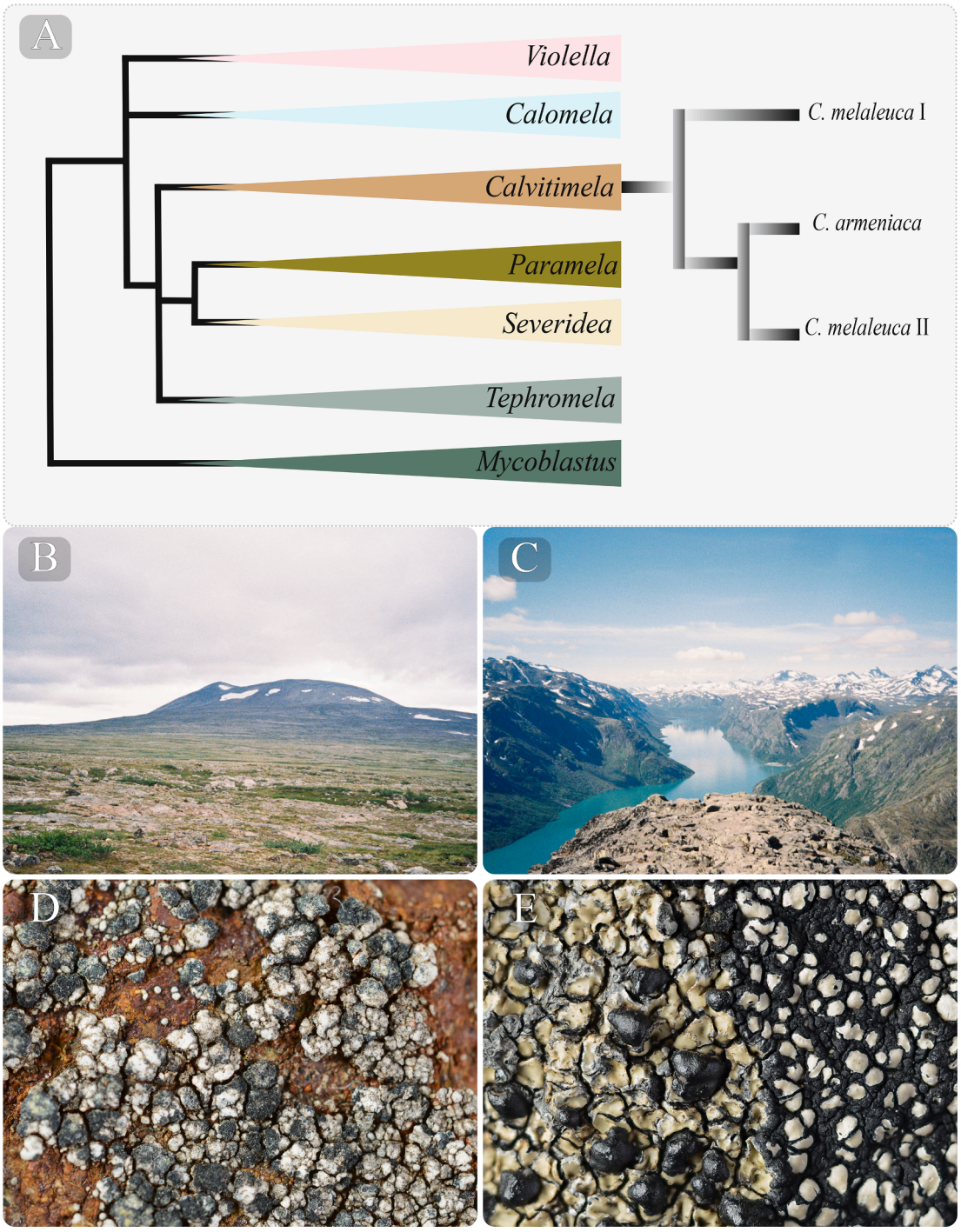

Fig. 1. Morphology, habitat, and phylogeny of Calvitimela. A. A schematic illustration of the phylogenetic relationships between the genera and subgenera in the Tephromelataceae (left), and between lineages in the subgenus Calvitimela (right), based on the results of Bendiksby et al. (2015). B-C. Typical habitats of the species in Calvitimela. D. Calvitimela cuprea (O-L-208192), E. C. melaleuca (O-L-228122 left, 228122 right).

further investigation and voucher deposition. In addition to our taxonomically broad sampling of *Calvitimela* s.lat., we also sampled *C. melaleuca* more densely at four selected localities from throughout Norway. The four localities were selected to get the widest possible geographic spread in Norway. At each locality, small thallus fragments were taken from 20 individuals (Table S2) within a radius of up to 5 m using a sterile knife.

Our taxon sampling outside *Calvitimela* is largely based on previous studies on the genera *Mycoblastus* (Spribille et al., 2011b), *Tephromela* (Muggia et al., 2008), and *Violella* (Spribille et al., 2011a). We used existing DNA sequence data from the three genera and included at least two vouchers per species to cover a large part of their known distribution range. Herein, we use the taxonomy of Bendiksby et al. (2015).

2.2. Morphology and chemistry

We examined the morphology of the material under dissecting microscopes. To properly assess thallus color, it was important to include a large proportion of fresh material, because color degrades over time in fungaria. When needed and available, type material was included

(Table S1). Ascospore (hereafter spore) size was measured for selected specimens (Table S1). Thin cross sections of apothecia showing individual asci were cut and placed in a drop of 5 % potassium hydroxide (KOH), and spore sizes were measured under light microscopes using immersion oil and 100X magnification. The spore size measurements were based on a single and suitable cross section (i.e., with at least 15 visible spores) from one apothecium per individual. All anatomically studied specimens were checked for crystals under polarized light. Amyloid reactions were tested after pretreatment with KOH, with a modified Lugol's solution, where water was replaced by 50 % lactic acid.

Thin-layer chromatography (TLC) was performed on nearly all included specimens of *Calvitimela* (see Table S1) in accordance with the methods of Culberson (1972), Menlove (1974), and Culberson & Johnson (1982). Secondary chemistry was examined using the solvent systems A (Menlove, 1974), B' (Culberson & Johnson, 1982) and C (Culberson, 1972) and run-on glass plates for identifying fatty acids.

2.3. Molecular data acquisition

We extracted genomic DNA from dried tissue (apothecia and/or thallus) using the E.Z.N.A plant kit (Omega Bio-tek, Inc., Norcross, Georgia, U.S.A.), following the manufacturer's guidelines except for a few modifications (as described by Bendiksby & Timdal, 2013). We continued with polymerase chain reaction (PCR) using Illustra PuReTaq Ready-To-Go beads (GE Healthcare, Buckinghamshire, UK) following the protocol described by Kistenich et al. (2018), with modified volumes for each reaction: 0.3 µl of both primers and a total mixture volume of 11.8 µl, to which 0.7 µl DNA template was added. The following nuclear genetic regions were amplified: the internal transcribed spacer region (ITS1, 5.8S, ITS2) with primers *ITS1F/ITS4* (White et al., 1990), and the large subunit (LSU) of the nuclear ribosomal rRNA with primers *LRlecF/LRlecR* (Schneider et al., 2015), the DNA replication licensing factor mini-chromosome maintenance component 7 (MCM7) with primers *Teph_mcm7F1/Teph_mcm7R2* (Bendiksby et al., 2015), and the translation elongation factor 1-α (TEF1-α) with the primers *Teph_tefF1/Teph_tefF1* (Bendiksby et al., 2015). Additionally, we amplified the mitochondrial ribosomal small subunit (mtSSU) using primers *mitSSU1/mitSSU3R* (Zoller et al., 1999), and internal primers (*mtSSU-RhiF, mtSSU-RhiR*; Möller et al., 2021. In prep.) when amplification was poor. The following PCR cycling conditions were used: 95 °C for 7 min, 35 cycles of 95 °C for 30 s, 58 °C for 30 s, 72 °C for 1 min, followed by 72 °C for 7 min. For the LSU marker slightly different cycling conditions were used: 95 °C for 7 min, 35 cycles of 95 °C for 30 s, 68–58 °C (touch down) for 30 s, 72 °C for 1 min, followed by 72 °C for 5 min.

We cleaned PCR products as described in Kistenich et al. (2018), with Illustra ExoProStar Clean-Up Kit (GE Healthcare, Buckinghamshire, UK), following the manufacturer's guidelines, except using a 10 × dilution of enzymes. The cleaned PCR products were sent for Sanger sequencing at Macrogen Europe (Amsterdam, The Netherlands) and the sample preparation was performed in line with the company's instructions.

2.4. Sequence curation, alignment, and model testing

We curated the sequences using Geneious Prime version 2020.1.2 (https://www.geneious.com/). An initial identity control was performed by searching our local BLASTn database (all lichen sequences in GenBank downloaded 2020-05-14 merged with all lichen sequences produced at O). We aligned sequences using Muscle (Edgar, 2004) in Aliview (Larson, 2014). To remove poorly aligned regions and make the trimming process reproducible we trimmed the alignments with Gblocks (Castresana, 2000; Talavera & Castresana, 2007) using the option for less stringent selection: allow gap position within the final blocks. The ITS sequences of *C. melaleuca* from the denser sampling in Norway aligned easily, and only the ends were manually trimmed away. Model testing was performed using PartitionFinder2 (Lanfear et al., 2016) applying the greedy algorithm (Lanfear et al., 2012), linked branch lengths and the starting Maximum Likelihood (ML) tree by PhyML (Guindon et al., 2010). Best fitting evolutionary substitution models were selected based on the small sample size corrected Akaike Information Criterion (AICc). The alignments of protein coding genes (MCM7 and TEF1-α) were partitioned according to codon positions, and the ribosomal marker (ITS) by the introns and ribosomal part (i.e., ITS1, 5.8S, ITS2). The alignments of the nuclear regions ITS, MCM7 and TEF1-α were concatenated applying the same partitions as described above.

2.5. Phylogenetic analyses

We constructed ML phylogenetic trees of individual alignments (ITS, LSU, MCM7, mtSSU, TEF1-α) and concatenated alignments (ITS + MCM7 + TEF1-α) with 10 random starting trees and 1000 bootstrap replicates using RAxML-NG-MPI v. 1.0.2. (https://github.com/amkozlov/raxml-ng/releases/tag/1.0.2; Kozlov et al., 2019). All gene alignments (except LSU and mtSSU) were also subjected to Bayesian inference using the mpi version of MrBayes 3.2.7a (github.com/NBISweden/MrBayes/ tree/v3.2.7a; Ronquist et al., 2012). Phylogenetic analyses were carried out on the computer cluster Bioint01 (bioint01.hpc.uio.no) at the University of Oslo. For the separate gene trees, the Metropolis-Coupled Markov Chain Monte Carlo (MC^3) was run for 10 million generations (12 for the concatenated and 8 for the *C. melaleuca* s. lat. alignment) with 4 separate chains and 4 individual runs sampling every 100th tree. Convergence and proper parameter mixing were assessed by inspecting trace plots in Tracer 1.7.1 (Rambaut et al., 2018), and by monitoring the value of the Average Standard Deviation of Split Frequencies (ASDSF) as the chains progressed. We assumed convergence of the chains when a value of ASDSF < 0.01 was reached. The burnin values for tree summarization were set manually at the nearest round generation (e.g., 1 million or 2.5 million) after the ASDSF value had dropped under 0.01. Bayesian gene trees were summarized using the *contype* option *allcompat*, whereas the trees inferred from the concatenated dataset were summarized using the *halfcompat* option to get a 50 % majority rule consensus tree.

Molecular dating was performed using a two-step secondary calibration. Firstly, a molecular dating was performed on a dataset of the major groups in the Lecanoromycetes using the DNA sequences of LSU and mtSSU retrieved from GenBank. Secondly, we performed a dating analysis on a subset of the Tephromelataceae data (see Table S1) excluding the outgroup and reducing the number of accessions in well sampled groups (i.e., *Severidea* and subgenus *Calvitimela*). In both calibration steps, ML phylogenies were inferred using the same methods as described above, except only partitioning by each genetic region (i.e., LSU, mtSSU and ITS, MCM7, TEF1-α). The ML topologies were transposed to ultrametric using the function *chronopl ()* in the package *ape* (Paradis & Schliep, 2019) in R version 4.0.3. (R Core Team, 2020) applying the calibrations described below. The software BEAUTi implemented in BEAST 2.6.3 (Bouckaert et al., 2019) was used for setting up all the molecular dating analyses. The different gene partitions were defined with unlinked substitution models, unlinked clock models and linked trees. The following substitution models were used for the Tephromelataceae data ITS: GTR + G, MCM7: TVMef + G and TEF1-α: SYM + I + G, and for the Lecanoromycetes data nLSU: GTR + I + G, mtSSU: TVM + I + G, setting the number of gamma categories to 4 and the number of invariant sites to be estimated. The ultrametric ML topologies were used as guiding tree topologies. We used four calibration points from Nelsen et al. (2020) in the initial analysis of the Lecanoromycetes dataset. Calibration priors were set by using the 95 % highest posterior density (HPD) intervals for the crown age estimates inferred by Nelsen et al. (2020). These were used as upper and lower bounds on uniformly distributed priors. The following initial secondary calibration priors were set: Lecanoromycetes 199.7–303.0 million years ago (Ma), Telochistales 76.9–151.8 Ma, Caliciales 50.3–167.1 Ma and Cladoniineae 36.8–85.8 Ma. Most recent common ancestor (MRCA) priors were applied to the crown node of the Tephromelataceae in the

first analysis and to the ingroup (all taxa except *Mycoblastus*) in the second analysis. We carried out two independent runs in BEAST 2.6.3 (Bouckaert et al., 2019) for both the Lecanoromycetes and Tephromelataceae data; one run with a log normal relaxed clock and one with a strict molecular clock. The age estimation (41.7–116.5 Ma) from the relaxed clock analysis on the crown node of Tephromelateaceae was used to calibrate the root node on the subset of the Tephromelataceae data (Table S1). For the Lecanoromycetes data the posterior was summarized with a maximum clade credibility (MCC) tree and median heights, using the software TreeAnnotator implemented in BEAST 2.6.3. Moreover, for the Tephromelataceae data, summarization was done onto the ultrametric ML topologies (see above) with both median and common ancestor heights (CA). All MCMC runs were run for 50 million generations, logging the trace and trees every 10^4th generation. We only discuss nodes relevant for answering the questions posited in this paper, specifically, excluding *Mycoblastus* and *Tephromela*.

We used Figtree 1.4.4 (https://tree.bio.ed.ac.uk/software/figtree/) to visualize and export tree files and pdfs for later editing in Adobe InDesign (Adobe Inc., 2020). Chemical and geographical characters were manually mapped on to the resulting phylogenies, in addition to bootstrap values from the ML analysis of the same dataset.

2.6. Data exploration and statistical analyses

The R environment was used for exploration of both the phenotypic (1) and molecular (2) data, respectively. (1) Spore size variation was investigated by plotting the mean width against the mean length for each observation (i.e., the mean of all 15 measurements for every individual measured) and fitting a line with the *stat_smooth ()* function implemented in *ggplot2* (Wickham, 2016) using the method "*loess*", and a value of 1.5 for *span*. To search for potential taxon-specific patterns ascribed to just spore length or spore width, boxplots for each were made by plotting the widths and lengths against taxa using *ggplot2* (Wickham, 2016). We performed a one-way ANOVA using *aov()* to assess significant differences in spore size (Table S6 & 8). Tukey Honest Significance Differences were computed with *TukeyHSD()* to give pairwise comparisons of all taxa with confidence intervals and significance values (Table S5-9). The normality assumption was checked with residual quantile–quantile (Q-Q) plots. The equal variance assumption was checked by inspecting scale location plots and performing the Levene's test (Table S10). (2) The haplotype network was constructed based on the parsimony criterion using the function *haploNet ()* in the R package *pegas* (Paradis, 2010). Substitution saturation was explored by plotting uncorrected genetic distances against corrected genetic distances using *dist.dna ()* in the package *ape*. For the corrected distances, the substitution model K80 (Kimura, 1980) was used with a gamma correction of distances as implemented in *dist.dna ()*. Linear regression analyses were performed with the function *lm ()* in R to test for the linearity between uncorrected and corrected genetic distances. The coefficient of determination of linear regression through the origin (R^2) was computed for the combined first and second codon position, the third codon position and the full loci for the protein coding genes. For ITS, R^2 was calculated for the combined variable regions ITS1 and 2, 5.8S and the full loci. Density plots of the distance matrices were created with *geom_density* in *ggplot2*, which implements the Kernel density estimation (KDE) to approximate the probability density function of the variable in question. The rationale behind including a saturation plot of ITS was to compare, between the nuclear markers, at which level of genetic distance substitutions occur. Segregating sites and base frequencies were calculated with the functions *seg.sites ()* and *base.freqs ()*, respectively, in the package *ape*.

3. Results

3.1. Morphology and chemistry

A morphological comparison between lineages in the subgenus *Calvitimela* uncovered a difference in thallus color between the two taxa *C. melaleuca* I and II (Fig. 2). The taxon *C. melaleuca* I exhibited white to occasionally light brown thallus color, whereas *C. melaleuca* II showed yellow to sometimes brownish-yellow thallus color. The specimens of *C. melaleuca* III had a thallus morphology resembling *C. armeniaca* more than *C. melaleuca* s. lat (i.e., *C. melaleuca* I and II), with beige colored thallus (not observed for the older specimen due to color degradation) with areolae edges becoming "melanin" pigmented and appearing black to dark gray.

We measured spore sizes for 32 specimens from different fertile *Calvitimela* species with five specimens per taxon, except *C. cuprea* (N = 2), *C. melaleuca* clade III (N = 2) and *C. perlata* (N = 4), including the lectotype of *C. melaleuca* (Fig. 2; Table S1). We observed significant differences ($p < 0.05$) in spore size between *C. perlata* and all other taxa (Fig. 2B; Table S5-9). The sister taxa *C. melaleuca* II and *C. armeniaca* had significantly narrower spores compared to the rest of the taxa, with only a few significant length differences (*C. melaleuca* II – *C. aglaea*, *C.* sp. – *C. armeniaca*, *C. melaleuca* II – *C. cuprea*; Table S5-9). The rest of the taxa had a general tendency to overlap in both spore length and width. Some specimens were misidentified in the field, or had incorrect names in GenBank, see the footnotes of Table S1 for a full list of these vouchers.

One newly discovered clade, *C.* sp., in *Severidea* (Fig. 3) containing atranorin and stictic acid (Fig. 2) was collected multiple times and in the field identified as *C. perlata*. In addition, two specimens (O-L-228131 and O-L-228193; Table S1) collected as *C. melaleuca* and *C. aglaea* respectively, were both fertile with whitish areolae. They contained identical chemistry as *C. cuprea* (Fig. 2) and likely represent a new, esorediate morphotype of the sorediate *C. cuprea* (Figs. 3 and 7).

Chemistry profiles were acquired from selected specimens (Figs. 2-4; Table S1-2; Supplementary information). In general, there was a lack of correlation between chemistries and phylogenetic clades (Fig. 4). The subgenus *Calvitimela* displayed a lot of variation in chemistry, with no chemical substances being diagnostic at the species level (Figs. 3-4). In *Severidea*, *C. aglaea* were easily distinguishable from the other species by containing bourgeanic acid and usnic acid (Fig. 3). The other species in *Severidea* were more similar, all sharing atranorin and stictic acid as major compounds. The two monotypic subgenera *Calomela* and *Paramela* were separated by the absence/presence of usnic acid (Fig. 3).

3.2. Molecular data

We generated a total of 301 sequences from 108 specimens: 171 from ITS (including 75 from the denser *C. melaleuca* sampling), 12 from LSU, 51 from MCM7, 13 from mtSSU, and 54 from TEF1-α (Table S1). Despite multiple attempts, we were not able to obtain sequence data of any of the loci for *C. austrochilensis*. We were, however, able to obtain one mtSSU sequence from an isotype of the Antarctic *C. uniseptata*.

3.3. Alignments and substitution models

The alignments consisted of 301 sequences produced during this study, 223 sequences mined from GenBank, and 2 unpublished sequences from the DNA database at O (Table S1-S2). The inferred substitution models differed amongst the loci and their partitions (Table S3). All alignments produced during this study are available as supplementary information (Supplementary data 1–5).

The saturation plots showed a linear relationship between uncorrected and corrected genetic distances for the combined first and second codon positions of MCM7 and TEF1-α (Fig. 5A). The most striking deviation from linearity was found at the third codon position for MCM7, reaching a substitution plateau at an uncorrected distance slightly below

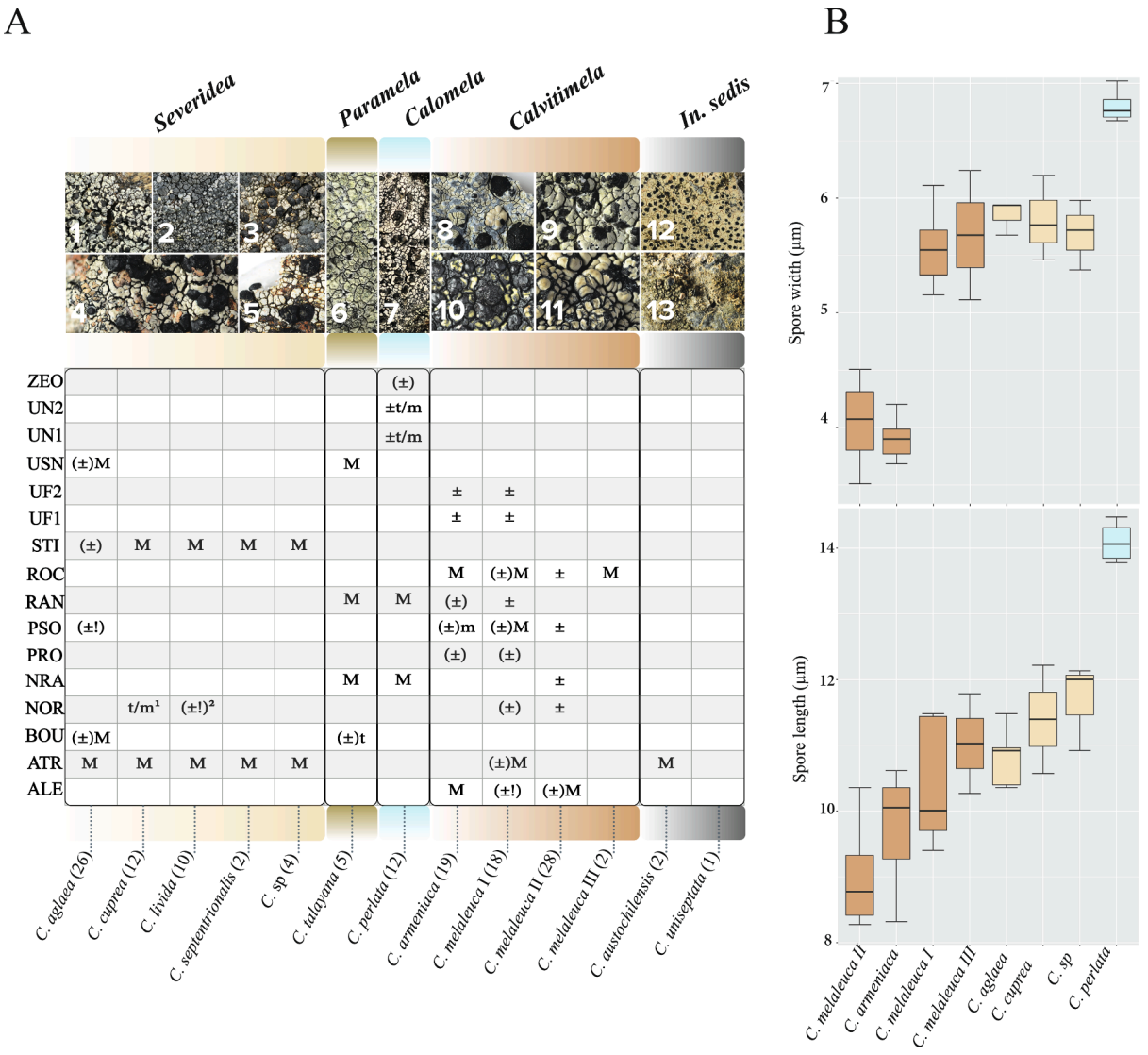

Fig. 2. Spore size and chemical variation in *Calvitimela*. **A.** Overview of the secondary metabolites occurring in *Calvitimela*. Abbreviations: ALE = Alectorialic acid, ATR = Atranorin, BOU = Bourgeanic acid, NOR = Norstictic acid, NRA = Norrangiformic acid, PRO = Protocetraric acid, PSO = Psoromic acid, RAN = Rangiformic acid, ROC = Roccellic acid, STI = Stictic acid, UF1 = Unknown fatty acid 1, UF2 = Unknown fatty acid 2, USN = Usnic acid, UN1 = Unknown substance 1, UN2 = Unknown substance 2. The following abbreviations indicate the degree of presence for the different lichen substances: M = major, m = minor, t = trace, ± = partly occurring, parentheses indicating rare occurrences and exclamation mark indicating very rare. [1]A single specimen of *C. livida* (O-L-228138) was found to contain norstictic acid, and [2]one specimen of *C. cuprea* (O-L- 228124) found to lack norstictic acid. Photos: **1**. *C. aglaea* (O-L-173831) **2**. *C. livida* (O-L-163835), **3**. sorediate *C. cuprea* (O-L-179616), **4**. *C.* sp (O-L-200938), **5**. esorediate *C. cuprea* (O-L-228131), **6**. *C. talayana* (O-L), **7**. *C. perlata* (O-L-163770), **8**. *C. armeniaca* (O-L-228166), **9**. *C. armeniaca* (O-L-228197), **10**. *C. melaleuca* II (O-L-225749), **11**. *C. melaleuca* I (O-L-225809), **12**. *C. austrochilensis* (MSC-0016623), **13**. *C. uniseptata* (UPS-L-838893). **B.** Spore length, and spore width boxplots showing the interquartile range of the data, with whiskers corresponding to the maximum and minimum values, and the centered black line corresponding to the median. The color coding corresponds to the different taxa.

0.6 with an R^2 of 0.327 (Fig. 5A). The density distribution of genetic distances varied across the different loci (Fig. 5B). Most notably, the absence of sequences with distances between 0.05 and 0.10 were observed for MCM7 and TEF1-α, whereas ITS had a higher density at this distance interval.

3.4. Gene tree topologies

The Bayesian MC^3 runs for the separate gene trees converged at slightly above 3 million generations (for ITS), slightly above 1.6 (for MCM7) and just below 1 million (for TEF1-α), all with effective sample size (ESS) values well above 200 for all parameters. The different gene trees (ITS, MCM7, TEF1-α) showed congruent topologies with respect to the major diverging lineages (Fig. S1) using ML, with no supported (greater than75 BS) incongruencies (Fig. S1). However, one TEF1-α sequence of *C. melaleuca* III was well-supported as sister to *C. armeniaca* and *C. melaleuca* II. Whereas the three ITS sequences from the same clade were well-supported as sister to *C. melaleuca* I. ITS had poor bootstrap support values (<60) in all deeper nodes of the topology. MCM7 had strong support for the ingroup/outgroup relationship (BS = 97) and intermediate support (BS = 75) for a monophyletic Tephromelataceae. TEF1-α showed near robust support (BS = 85) for ingroup/outgroup and low support (BS = 68) for a monophyletic Tephromelataceae. All gene trees share an important feature, intermediate branch lengths are short and generally with low bootstrap support. The Bayesian gene trees of ITS and TEF1-α, by comparison, showed much higher support (PP) among these short branches at intermediate to deep topological levels. MCM7 however, showed similar branch support (PP) to bootstrap resampling with only a small to moderate overall increase in PP's at all internodes.

Due to low PCR success rate and the unclear phylogenetic signal from

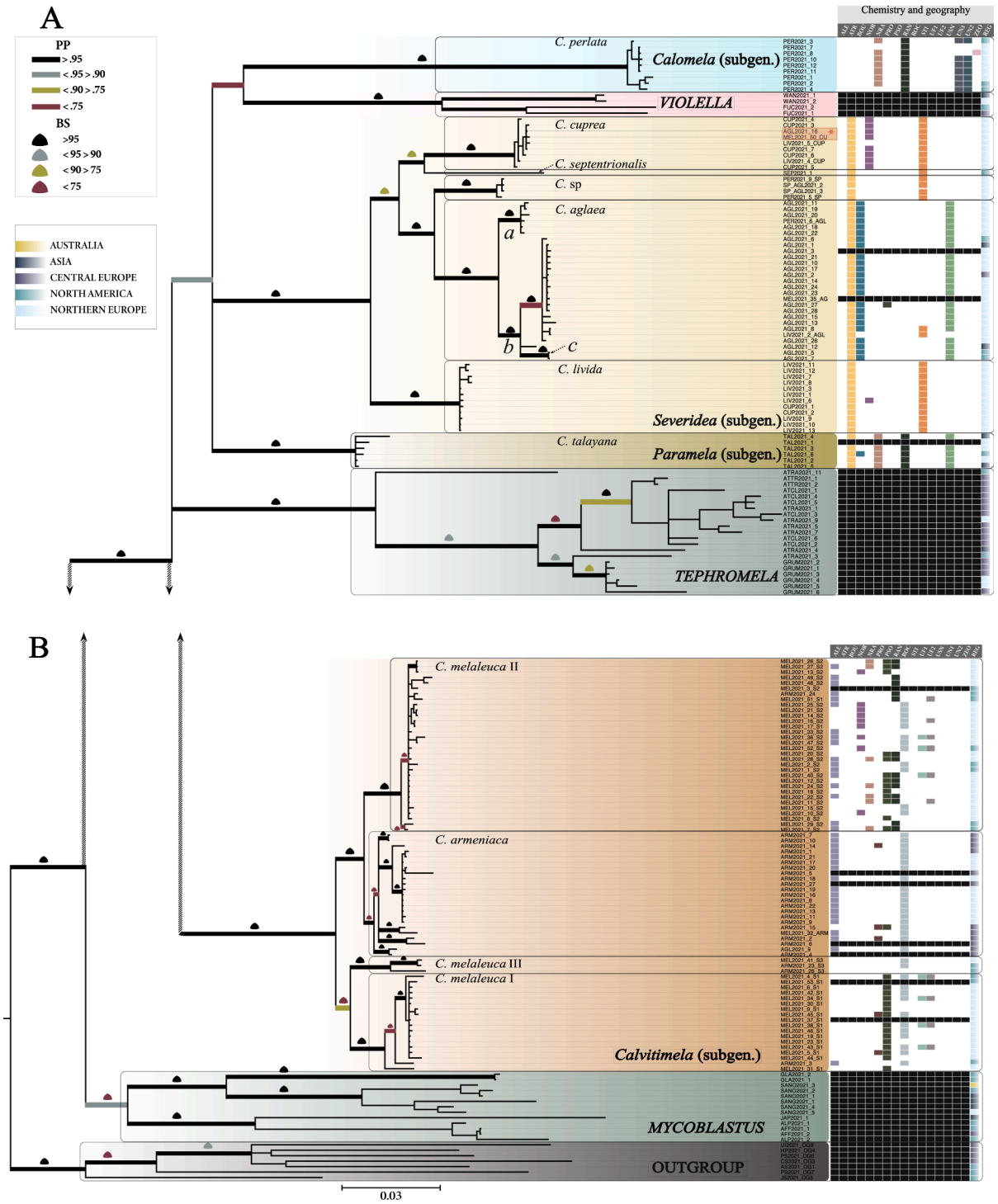

Fig. 3. Phylogeny, chemistry, and geography of *Calvitimela*. **A-B.** Bayesian 50 % majority rule consensus tree based on 183 accessions and 1794 aligned characters from the concatenated nuclear regions (ITS, MCM7, TEF1-α). Thick branches with different colors indicate posterior probabilities (PP; see figure legend). Bootstrap values from 1000 replicates are shown with colored triangles (see figure legend). Triangles for short branches in the subgenus *Calvitimela* are scaled down to reduce overplotting. The different color codes indicate the separate genera and subgenera in the Tephromelataceae. Major geographical zones are manually mapped on the phylogeny with different colors (see figure legend). The nodes "a", "b", and "c" highlight three supported groupings within the species *C. aglaea*. The chemistry of vouchers from *Calvitimela* are mapped onto the phylogeny with different colors in the right-hand matrix. The black squares indicate vouchers for which no TLC data was obtained. Abbreviations for the different lichen substances: ALE = Alectorialic acid, ATR = Atranorin, BOU = Bourgeanic acid, NOR = Norstictic acid, NRA = Norrangiformic acid, PRO = Protocetraric acid, PSO = Psoromic acid, RAN = Rangiformic acid, ROC = Roccellic acid, STI = Stictic acid, UF1 = Unknown fatty acid 1, UF2 = Unknown fatty acid 2, USN = Usnic acid, UN1 = Unknown substance 1, UN2 = Unknown substance 2. The last column shows the different regions of origin for the included vouchers (abbreviation REG = Region; see figure legend). The scale bar indicates the number of substitutions per site. The two accessions of the esorediate and fertile morphotype of *C. cuprea* are highlighted in red. (For interpretation of the references to color in this figure legend, the reader is referred to the web version of this article.)

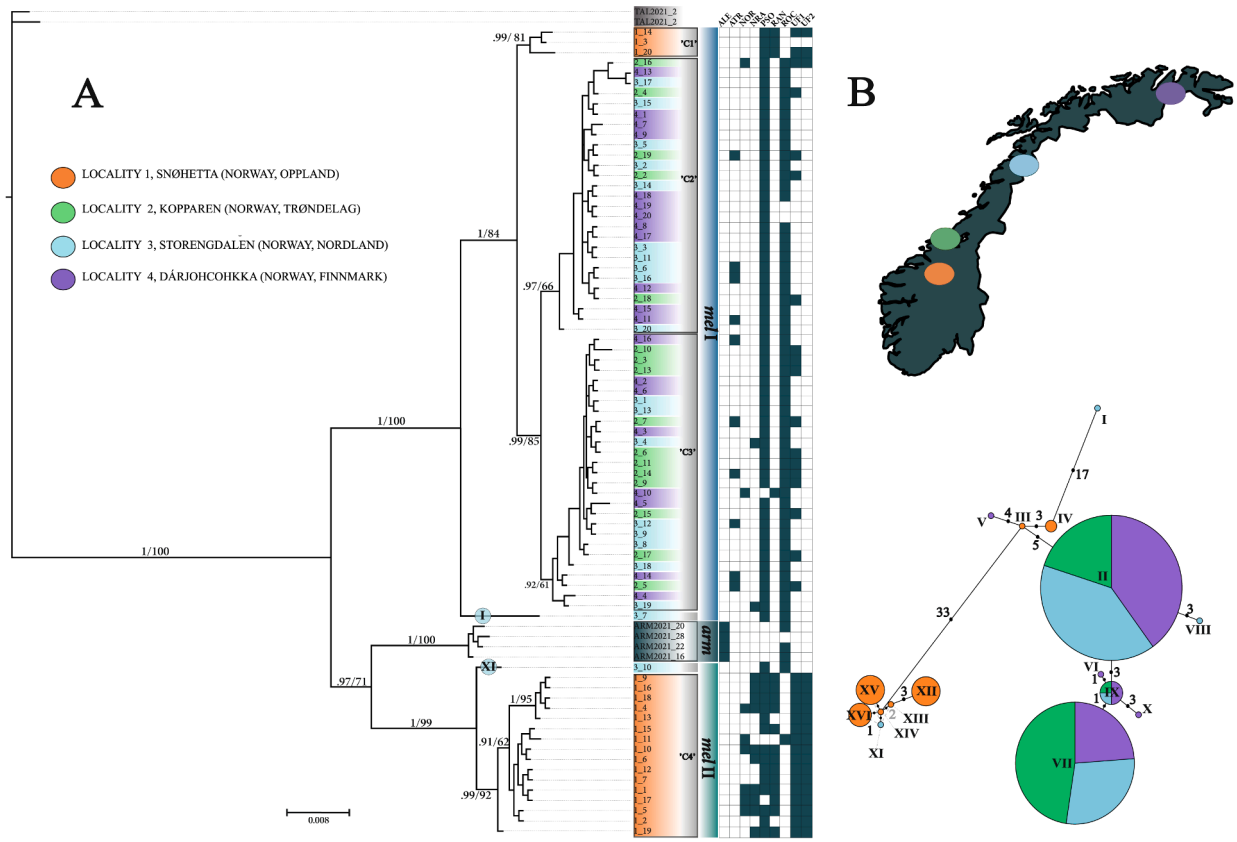

Fig. 4. Distribution and genetic structure of *C. melaleuca* s. lat in Norway **A.** A Bayesian majority rule consensus phylogram of the ITS of *C. melaleuca* s. lat. across Norway (see figure legend). Branch support values are shown above branches as posterior probabilities (PP)/Bootstrap support (BS; manually mapped onto the Bayesian topology) with the scale bar indicating number of substitutions per site. Individual branches are colored with respect to their geographical origin (see figure legend), and the three groups arm, mel I and II are indicated with blue, dark gray and green, respectively. The four different subclades of *C. melaleuca* s. lat. are indicated with 'C1′ through 'C4′. From locality 3, two individuals represent outliers in mel I (haplotype I and XI). The chemistry of individual population samples is mapped onto the phylogeny. Abbreviations for the different lichen substances: ALE = Alectorialic acid, ATR = Atranorin, NOR = Norstictic acid, NRA = Norrangiformic acid, PSO = Psoromic acid, RAN = Rangiformic acid, ROC = Roccellic acid, UF1 = Unknown fatty acid 1, UF2 = Unknown fatty acid 2. **B.** Map showing the different localities where 20 individuals of *C. melaleuca* were sampled. Haplotype network of *C. melaleuca* based on the ITS. There were 16 haplotypes recovered in the analysis, each circle representing a unique haplotype with corresponding roman numerals, and size indicating haplotype frequency. Distances between nodes indicate the number of mutations. Circles are colored by sampling-locality (see figure legend). (For interpretation of the references to color in this figure legend, the reader is referred to the web version of this article.)

the mtSSU, we were unable to present a reasonable interpretation of these sequences (Fig. S2A). However, our phylogenetic analyses strongly support the accession of *C. uniseptata* to belong in the genus *Lecania* (Ramalinaceae; Fig. S3). We experienced multiple copies of the LSU in the PCR products during gel electrophoresis with all *Calvitimela* amplicons. The possibility of paralogy or presence of DNA from other lichen-associated fungi prevented us from making rational comparisons of phylogenetic relationships shown by these loci (Table S1; Fig. S2B).

3.5. Concatenated topology

The Bayesian MC^3 runs converged at just below 8 million generations, with ESS values well above 200 for all parameters. The deeper nodes in the Tephromelataceae were unresolved (Fig. 3). All included genera and subgenera were highly supported, respectively, except for a moderately supported *Mycoblastus* (BS = 64). Their interrelations, however, remain largely unresolved and unsupported by bootstrapping. A clade of *Calvitimela* subgenera *Calomela*, *Paramela*, and *Severidea*, and the genus *Violella*, was supported only moderately by posterior probability (PP = 0.92). A sister-relation between *Calomela* and *Violella* was only marginally supported by posterior probability (PP = 0.5).

Our phylogenetic analyses of the concatenated data showed four independent lineages in the subgenus *Calvitimela* (Fig. 3). Firstly, a new highly supported clade *C. melaleuca* III (BS = 100, PP = 1), was recovered as sister to *C. melaleuca* I (BS = 100, PP = 1) with marginal to moderate support (BS = 55, PP = 0.85). Secondly, the partly supported clade *C. armeniaca* (BS = 61, PP = 0.96) was indicated as sister to the *C. melaleuca* II clade (BS = 100, PP = 1) with high support (BS = 99, PP = 1). Within C. *armeniaca* six fully supported (BS = 100, PP = 1), relatively short to intermediate length branches were recovered. There was a topological discordance between the gene trees and the tree based on the concatenated data in the subgenus *Calvitimela*. However, only one relationship was supported (see above: 3.4). Another highly supported lineage (*C.* sp; BS = 100, PP = 1) was recovered as a sister taxon to *C. aglaea* (BS = 100, PP = 1) with high support (BS = 97, PP = 1). Within *C. aglaea*, three groupings were recovered with high support (BS = 100, PP = 1; Fig. 3: node "a", "b" and "c"), and one moderately supported grouping (BS = 100, PP = 78; Fig. 3: node "d"). A single accession of *C. septentrionalis* grouped as a moderately to highly supported sister (BS = 84, PP = 1) to *C. cuprea*. With collapsed topological edges of the ML tree, based on the concatenated data (setting a cutoff at bootstrap values < 75), the backbone of the lineages *Calvitimela*, *Calomela*, *Tephromela*, *Severidea*, *Paramela* and *Violella* were reduced to a polytomy.

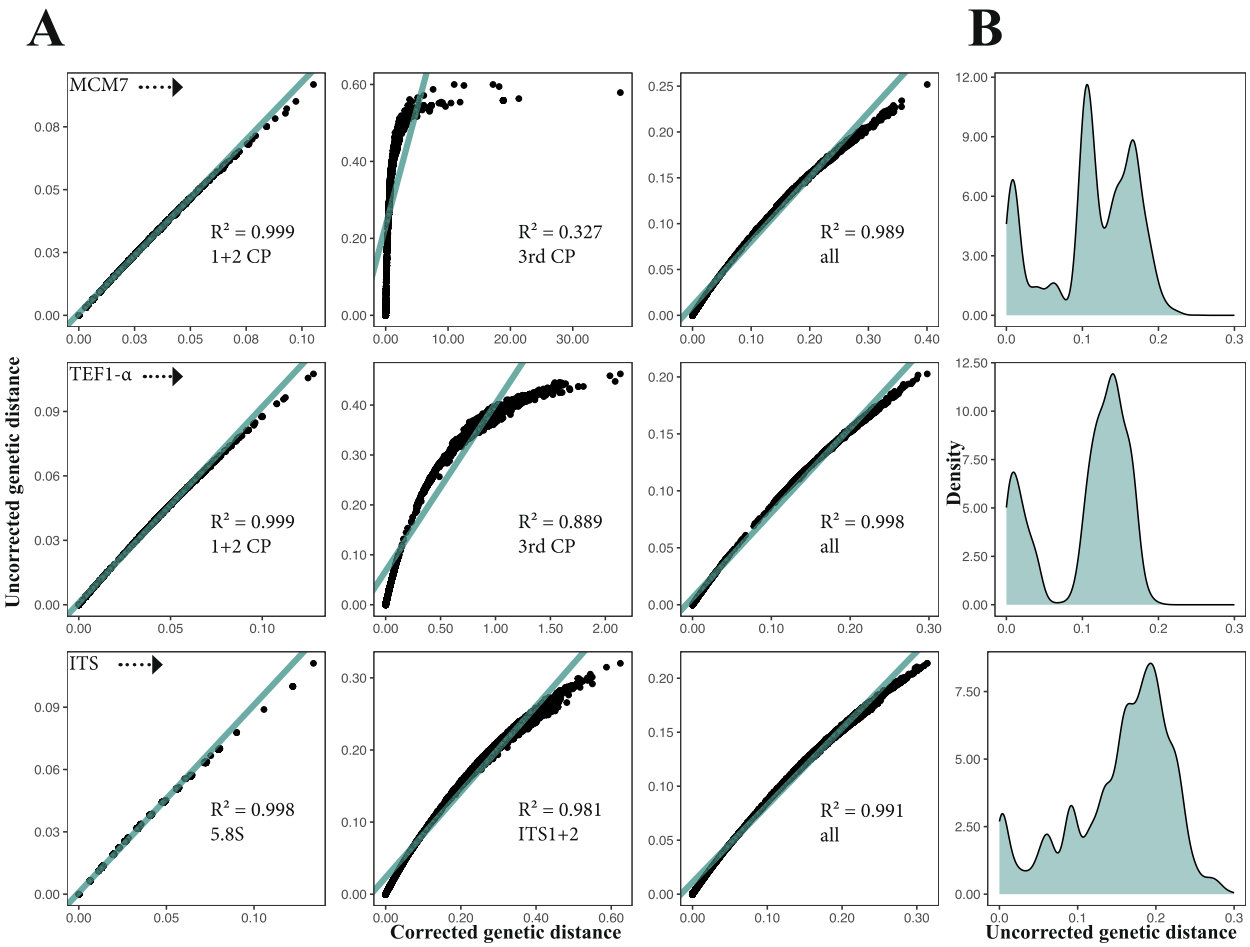

Fig. 5. Substitutional saturation and density of genetic distances. **A.** Saturation plots of the three nuclear alignments with outgroup taxa excluded, from the top: MCM7, TEF1-α, and ITS. The plots show the uncorrected (raw) genetic distances as a function of K80 gamma corrected distances. For the two loci MCM7 and TEF1-α, the first and second codon position (1 + 2) are shown first (left column) followed by the third codon position (middle column). For ITS, the 5.8S region is shown first (left column) followed by the two variable regions, ITS1 and ITS2 (middle column). Saturation plots for the loci in their entirety are shown in the right column. **B.** Density plots of the uncorrected (raw) genetic distances for the three nuclear loci. The plot shows the approximated probability density function of genetic distance through the Kernel density estimation (KDE).

3.6. *C. melaleuca* in Norway

The Bayesian MC^3 runs for the population (ITS) analysis converged at approximately 500 000 generations, with ESS values above 200 for all parameters. The two main lineages of *C. melaleuca* (mel I and mel II; (corresponding to the clades *C. melaleuca* I and II in Fig. 3) were recovered with robust support by both Bayesian and ML phylogenetic analyses (Fig. 4). The lineage representing *C. armeniaca* was recovered as the sister taxon to *C. melaleuca* II (mel II). However, the monophyly of *C. armeniaca* + *C. melaleuca* II was only partially robust (PP = 0.97, BS = 71), as also indicated in the concatenated topology (Fig. 3). Sixteen different haplotypes of ITS were recovered across all sampled individuals with the two most abundant (II and VII) were exclusive to mel I. A total of five samples corresponding to clade 'C1′ and two outlier branches in mel I and mel II, respectively, showed unexpected phylogenetic placements (see Fig. 4; Table S2). The three individuals in the clade 'C1′ grouped close to mel I and not mel II as the rest of the samples from the same locality. The ITS sequences of these three individuals showed 37 shared characters (nucleotides out of 556–6.7 % difference) that differed from the three individuals compromising *C. melaleuca* III (in Fig. 4).

3.7. Molecular dating

The two MCMC runs from one strict and one relaxed molecular clock analysis converged with ESS values above 200 for all parameters. The two different dating analyses showed incongruent backbone topologies with differences in supported branches (Fig. 6; Table S4). Negative branch lengths were observed at the short branches leading up to *Calomela*, *Paramela* and *Violella* in the resulting tree from the strict molecular clock analysis. These were mitigated with CA height summarization. The median age estimates differed between the strict and relaxed molecular clock analysis, but 95 % HPD intervals were overlapping (Fig. 6; Table S4). From the relaxed molecular clock analysis, the estimated median age for the split leading up to *Calvitimela* s. lat and *Violella* was 34.85 Ma (26.14–58.70 Ma 95 % HPD). While the divergence between *Severidea* and the lineages *Calomela*, *Paramela* and *Violella* was 32.79 Ma (24.40–54.30 Ma 95 % HPD).

Within *Severidea*, *C. livida* was estimated to have diverged from the rest of the taxa in this subgenus 10.83 Ma (7.35–18.33 Ma 95 % HPD). The subsequent split between *C. cuprea* and *C. aglaea* + *C.* sp. was estimated at 8.68 Ma (5.81–14.76 Ma 95 % HPD). Furthermore, the split between *C. aglaea* + *C.* sp. was estimated at 5.89 Ma (3.47–10.29 Ma 95 % HPD), and the estimated time between *C. cuprea* and *C. septentrionalis* 5.65 Ma (2.14–10.21 Ma 95 % HPD). Between the two groupings "a" and "b" within *C. aglaea* the estimated node age was 3.08 Ma (1.91–5.38 Ma

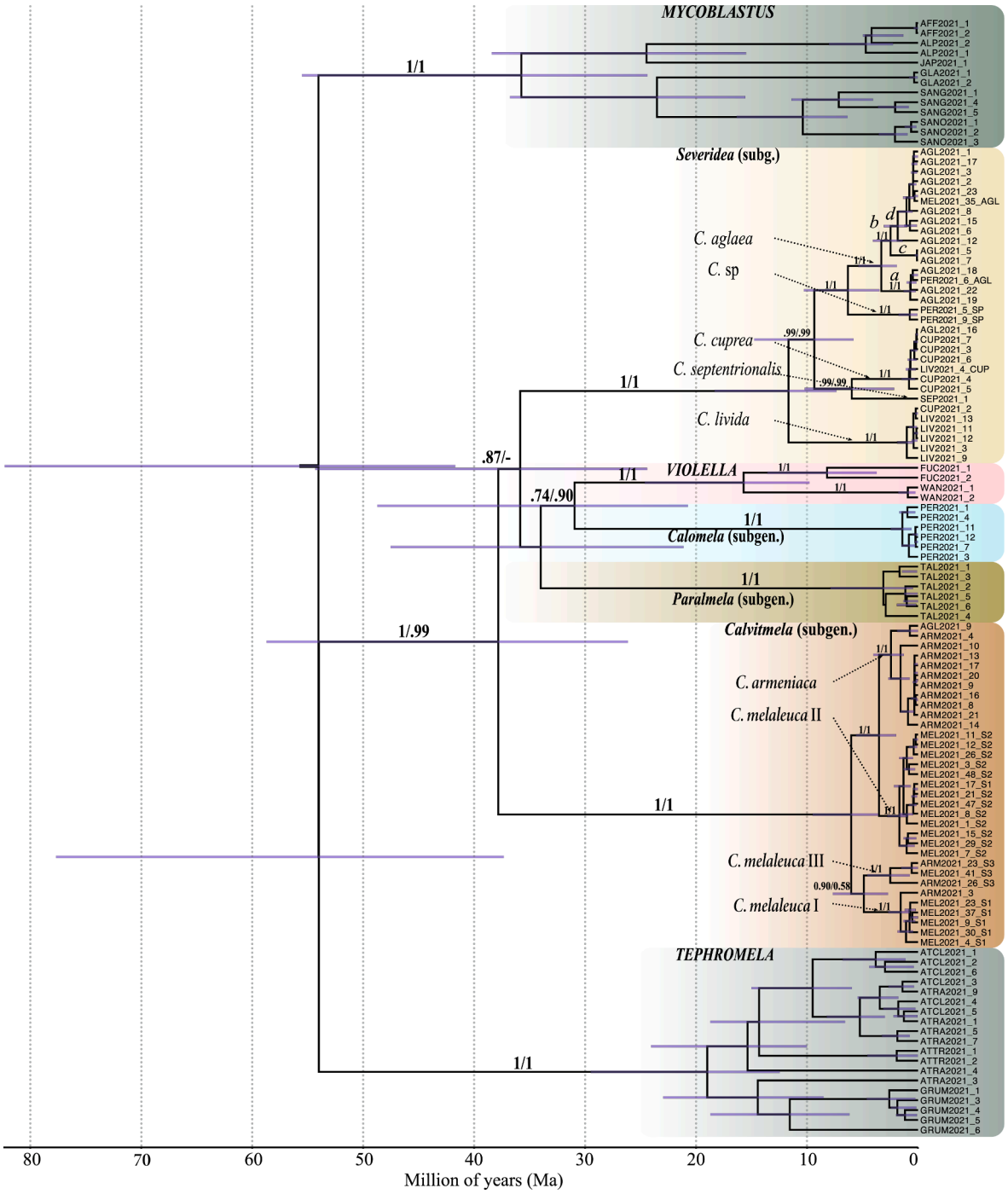

Fig. 6. Time calibrated phylogeny of the Tephromelataceae. A Bayesian common ancestor chronogram from the relaxed clock molecular dating analyses of three nuclear loci ITS, MCM7 and TEF1-α. Clade coloring represents the different genera and subgenera in the Tephromelataceae. The different lineages of *Calvitimela* are indicated with dotted arrows. The scale axis at the bottom represents age in millions of years (Ma). Node bars indicate the 95 % highest density posterior interval (95 % HPD) for estimated node ages (Ma). Posterior probabilities from the relaxed (in black) and strict (in gray) molecular clock analyses are shown above branches.

95 % HPD).

The estimated node age for the ancestral node to the lineages within the subgenus *Calvitimela* was 5.61 Ma (3.58–9.50 Ma 95 % HPD). Whereas the split between *C. armeniaca* and *C. melaleuca* II was estimated to 3.28 Ma (1.97–5.59 Ma 95 % HPD). The split between *C. melaleuca* I and III was estimated to 4.44 Ma (2.70–7.68 Ma 95 % HPD). The two different molecular dating analyses showed high support for the monophyly of *Calvitimela* s. lat + *Violella*. All major lineages corresponding to genera and subgenera were recovered as in previous analyses (see Table S4).

4. Discussion

4.1. Paraphyly, character state incongruence, and taxonomic implications

Our phylogenetic analyses of the three nuclear loci revealed deeply divergent and strongly supported clades with unclear relationships to each other in the family Tephromelataceae (Figs. 3 and 6), echoing the findings by Spribille et al. (2011a) and Bendiksby et al. (2015). This study further infers that the strongly supported and long-branched subgenera within *Calvitimela* s. lat., and the genus *Violella,* diverged

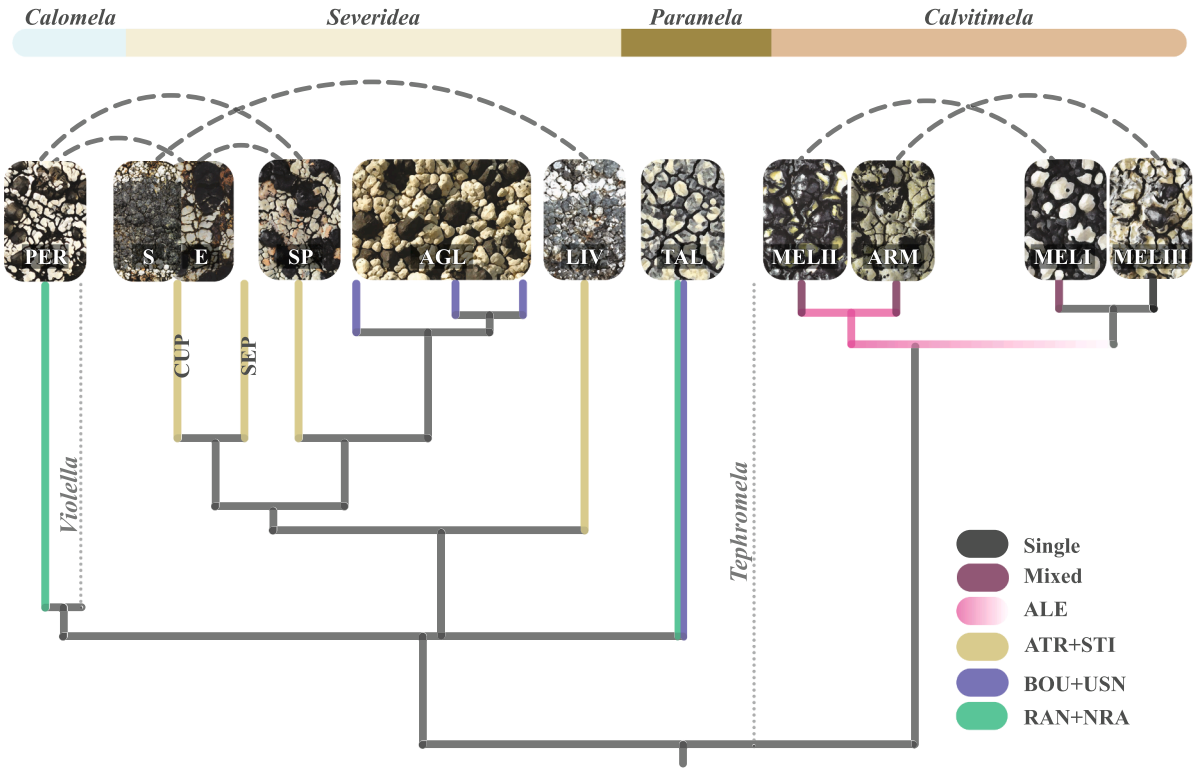

Fig. 7. Patterns of cryptic diversity in *Calvitimela*. A schematic display of the major trends in chemistry and morphology in relation to the molecular phylogeny. Dotted lines show taxa with similar macro-morphology and colored branches represent major trends in chemistry. Chemistry abbreviations: Single = taxon with only a single detectable compound, here only *C. melaleuca* III with roccellic acid, Mixed = taxa with highly variable and non-diagnostic compounds, ALE = alectorialic acid, ATR + STI = atranorin + stictic acid, BOU + USN = bourgeanic acid + usnic acid, RAN + NRA = rangiformic acid + norrangiformic acid. Taxon abbreviations (left to right): PER = *C. perlata*, CUP = *C. cuprea* (E = esorediate, S = sorediate), SEP = *C. septentrionalis*, SP = *C.* sp., AGL = *C. aglaea*, LIV = *C. livida*, TAL = *C. talayana*, MELII = *C. melaleuca* II, ARM = *C. armeniaca*, MELI = *C. melaleuca* I, MELIII = *C. melaleuca* III.

about 35 Ma (Fig. 6; Table S4), suggesting that they represent relatively old evolutionary lineages. Rapid diversification is known to blur phylogenetic relationships as the short divergence time does not allow enough substitutions to sort into the respective lineages (e.g., Widhelm et al., 2019). Given the short branch lengths at the time during which the subgenera diverged renders incomplete lineage sorting (ILS: i.e., the retention of ancestral polymorphism) in deep time a possible explanation (see Alda et al., 2019). Alternatively, or additionally, substitutional saturation may have caused underestimated divergence and homoplasy (Philippe et al., 2011; Widhelm et al., 2019; see section 4.5 below). These phenomena are increasingly common for deeper divergences (Delsuc et al., 2005).

Our results also show incongruence between the molecular phylogeny and morphological characters and provide evidence for the insufficiency of chemical characters as diagnostic tools in *Calvitimela* (Figs. 2, 3, and 7). Monophyly of *Calvitimela* s. lat. is not supported by our expanded molecular phylogeny. This, despite the fact that the black, shiny and lecideine apothecia and the blue-green color of the epithecium (e.g., Haugan & Timdal, 1994) makes them distinct from members of the genera *Mycoblastus*, *Tephromela*, and *Violella*. Although species of *Mycoblastus* and *Violella* also have lecideine apothecia, they are epiphytic and have several anatomical traits that distinguish them from *Calvitimela* s. lat. (see Spribille et al., 2011a, b; Kantvilas, 2009). It has recently been suggested that an inherent mismatch between the lichen phenotype and its corresponding fungal molecular phylogeny often exists (Spribille et al., 2018). This stems from the realization that lichens achieve their phenotype through the symbiotic state. The evolution of one symbiont (the fungal component) seems to not always explain the observable phenotypic outcome of a lichen. Currently, there are no available sequences for photobionts in *Calvitimela*, and we cannot exclude that symbiont interaction may influence phenotypic outcomes.

Two species of *Calvitimela*, *C. uniseptata* and *C. austrochilensis*, appear to be extraneous in the Tephromelataceae. The mtSSU from the single accession of *C. uniseptata* group (with high support) in the genus *Lecania* A. Massal. (Fig. S3), more specifically in an Antarctic clade within *Lecania* (see Næsborg et al., 2007). From its description by Thor (in Lumbsch et al., 2011), *C. uniseptata* has a squamulose thallus and a single septum in its spores. These morphological features indeed fall within the concept of *Lecania* s. lat. We suggest that either a combination into *Lecania* or alternatively synonymizing it with *L. brialmontii* (Vain.) Zahlbr., would be an appropriate taxonomic conclusion for *C. uniseptata*. The inability to amplify the markers TEF1-α and MCM7 from *C. austrochilensis* and *C. uniseptata*, using Tephromelataceae specific primers, strengthens the case that *C. austrochilensis* may also be extraneous to the family Tephromelataceae. However, as amplification was difficult with most primers for specimens of old age and the fact that the *C. austrochilensis* specimen was collected back in 1969, no conclusions can be drawn based on amplification failure alone.

Current modern classification practices aim at accommodating monophyletic taxa. Because *Calvitimela* cannot be shown monophyletic with the current data, any taxonomic decision at the generic level would include either accepting a seemingly paraphyletic genus *Calvitimela*, which would be status quo, or reaccepting a *Tephromela* sensu Hertel & Rambold (1985). The latter would imply lumping all species in *Calvitimela*, *Tephromela* and *Violella* into one large and morphologically heterogeneous *Tephromela*, as discussed by Spribille et al. (2011a). A third solution would be to recognize all the long-branched and strongly supported clades as separate genera and thereby raise the taxonomic rank of the current *Calvitimela* subgenera. Such a classification would indeed reflect evolutionary history and accommodate the suggested temporal band for generic circumscription in the Parmeliaceae suggested by Divakar et al. (2017). Such a solution would, however, render several

monotypic genera, which is at odds with "good taxonomic practice". More problematic is that it would make it impossible to assign some individuals to the correct genus without specialized equipment.

4.2. Subgenus Calvitimela: Diversification and complex chemistry

Our phylogenetic results show four supported clades in subgenus *Calvitimela* corresponding to *C. armeniaca*, *C. melaleuca* I, *C. melaleuca* II and *C. melaleuca* III (Fig. 3A-B). The three former were recognized also by Bendiksby et al. (2015), whereas *C. melaleuca* III is recognized for the first time herein. Thus, the name *C. melaleuca* currently refers to three distinct evolutionary lineages that, as currently circumscribed, are paraphyletic with respect to *C. armeniaca*.

In subgenus *Calvitimela*, no aromatic substances or fatty acids appear to be clade specific, meaning they are neither completely absent nor fully present in any single clade, despite strong molecular support. This result presents a major obstacle for using chemistry as an identification tool for these species (Figs. 2, 3, and 7). All compounds overlap between at least two clades and most overlap between all, such as for example alectorialic acid and roccellic acid. Nevertheless, the overall chemosyndrome in the subgenus is informative as it is unquestionably distinct from the other subgenera in *Calvitimela*. The idea that the expression of secondary metabolites can change due to ecological factors (e.g., Färber et al., 2014; Asplund et al., 2017) presents exciting grounds for testing hypotheses. The subgenus *Calvitimela* would serve as an interesting model to explore questions about how altitudinal or substrate gradients influence the chemosyndromic outcome in crustose lichens.

The three clades of *C. melaleuca* s. lat. have overlapping morphologies, but thallus color seems to be diagnostic for fresh material, in which *C. melaleuca* I is white to light brown, *C. melaleuca* II yellow to brownish-yellow, and *C. melaleuca* III beige. We find it highly interesting that the *C. armeniaca* morphology shows up in the newly discovered clade *C. melaleuca* III (Fig. 7). This is an example of similar phenotypic outcomes in two divergent fungal lineages (discussed by Spribille, 2018). This may be the result of different symbiont compositions (in *C. armeniaca* and *C. melaleuca* III) as previously reported for several other lichens (Ertz et al., 2018; Steinová et al., 2022).

Calvitimela melaleuca I seems to be the most widely distributed clade in Norway (Fig. 4). However, *Calvitimela melaleuca* II and the subclade 'C1′ originated from the only high-altitude locality (locality 1, Snøhetta above 2000 masl in a high alpine area; Table S2). These clades, together with *C. armeniaca*, appear to be connected to higher elevations, and have smaller spore sizes compared to the other clades in the subgenus (Fig. 2). The more phylogenetically derived position of clades 'C2′ and 'C3′ may indicate that the common ancestor of subgenus C*alvitimela* was a high elevation species from which low-land lineages have derived. As the genetic lineages of the *C. melaleuca* s. lat. appear to have diverged rather recently (Fig. 6), the lack of correlation between phylogenetic clades and geographic distance may be explained by ILS (see Garrido-Benavent et al., 2021). Multilocus data may be able to elucidate ILS further.

4.3. Subgenus Severidea: Intraspecific variation and new observations

According to our phylogenetic hypothesis, subgenus *Severidea* consists of five clades corresponding to the species *C. aglaea*, *C. cuprea*, *C. livida*, *C. septentrionalis*, and one hitherto unknown species (*C.* sp.; Fig. 3A). The specimens of this new species were collected as *C. perlata*, which was assigned by Bendiksby et al. (2015) to its own subgenus (*Calomela*). Despite its morphological resemblance to *C. perlata*, our phylogenetic results show that the new species is highly supported as a phylogenetic sister to *C. aglaea*. Both chemistry and spore measurements support its classification in subgenus *Severidea* (Fig. 2). Moreover, the new species is estimated to have diverged from *C. aglaea* about 6 Ma (Fig. 6; Table S4), strengthening the conception of this as a distinct evolutionary lineage that could be considered for recognition at the species level.

Our phylogenetic results corroborate that *C. aglaea* is genetically heterogeneous with three highly supported groupings (Fig. 3A: "a", "b", and "c") and one moderately supported grouping ("d"). Hence, with our wider sampling of *C. aglaea* (27 vs 15), the same clades are evident as in the molecular phylogeny by Bendiksby et al. (2015). Our crown group estimate of *C. aglaea* is about 3 Ma (Fig. 6), and clades "c" and "d" diverged around 2.3 Ma (Fig. 6). Compared to the estimated divergence time for *C. armeniaca* from *C. melaleuca* II (ca. 3.28 Ma), the "aglaea" divergence times suggest recognition as subspecies, if not at species level. Prior to taxonomic conclusions, this heterogeneous species should be subjected to comprehensive morphological investigations to elucidate potential phylogenetically informative phenotypic differences.

Our detection of an esorediate and fertile morphotype of *C. cuprea* (Fig. 8) implies an extension of the morphological range of this species as it was defined by Bendiksby et al. (2015). Different morphotypes with respect to reproductive characters are not uncommon for lichen species (see Lumbsch and Leavitt, 2011). Dispersion by vegetative propagules, such as soredia, is thought to represent a selective advantage in stable environments and during population establishment (Singh et al., 2015b). In our molecular data, there is no correlation between supported molecular topology and the reproductive strategies of the specimens (Fig. 3A), providing no indication of a lichen species pair in *C. cuprea* (see Poelt 1970; Mattson & Lumbsch, 1989). Another, less likely, explanation we can think of for the seemingly non-random distribution of reproductive strategies in this species includes photobiont switching, which was recently shown for a similarly dimorphic pattern in *Lecanographa amylacea* (Ehrh. ex Pers.) Egea & Torrente (Ertz et al., 2018). This flexibility in photobiont choice seems to allow the lichen to better withstand variable environmental conditions, and thereby help the lichen species in widening its distribution (Ertz et al., 2018). The two species *C. cuprea* and *C. livida* would by most lichenologists be regarded as phenotypically cryptic with relation to each other. Yet, our molecular dating estimates suggest that the two species shared a common ancestor as far back as almost 11 Ma (Fig. 6; Table S4). They differ slightly in chemistry, with *C. cuprea* having a trace of norstictic acid (Bendiksby et al., 2015). Surprisingly, one specimen of *C. cuprea* was found to lack norstictic acid and one specimen of *C. livida* to contain norstictic acid (Table S1). This questions the chemical distinction previously held between *C. cuprea* and *C. livida* by Bendiksby et al. (2015). Their ecologies are also different, with *C. cuprea* being associated with heavy metal rocks in old copper or nickel mines, and *C. livida* having a wider habitat range. Although this ecological distinction may be important, it is not fully diagnostic, as several *C. cuprea* individuals have been collected outside of mining habitats (e.g., Lendemer & Harris, 2016). That said, *C. cuprea* seems to have a greater affinity towards growing on rocks rich in heavy metals, supposedly with preferences towards copper.

4.4. Cryptic diversity and practical species concepts

The observed phenotypic similarity between non-monophyletic and more distantly related clades (i.e., *C. cuprea* vs. *C. livida*, *C. sp.* vs. *C. perlata*, *C. sp.* vs. the esorediate morphotype of *C. cuprea*, and *C. melaleuca* I vs. II; Figs. 2, 3, and 7) may represent parallel or convergent adaptations to similar environments (see Lumbsch and Leavitt, 2011). An interesting observation for the abovementioned clades is that even if they are similar in morphology, they seem to differ at some level between pairs. For example, the larger spore size in *C. perlata* distinguishes it from all other taxa in *Calvitimela* s. lat. Hence, even though *C. perlata* seems to be cryptic in a macro-morphological sense, we show that it is readily distinguishable based on at least one anatomical character. Moreover, subtle differences in chemistry, such as those between *C. cuprea* and *C. livida*, or in thallus color like the ones between *C. melaleuca* I and II, seemingly argues against the presence of cryptic species sensu Struck et al. (2018a) in *Calvitimela*. However, the degree and frequency of overlap in chemistry and morphology, increases the chances of misidentifications, especially in the field.

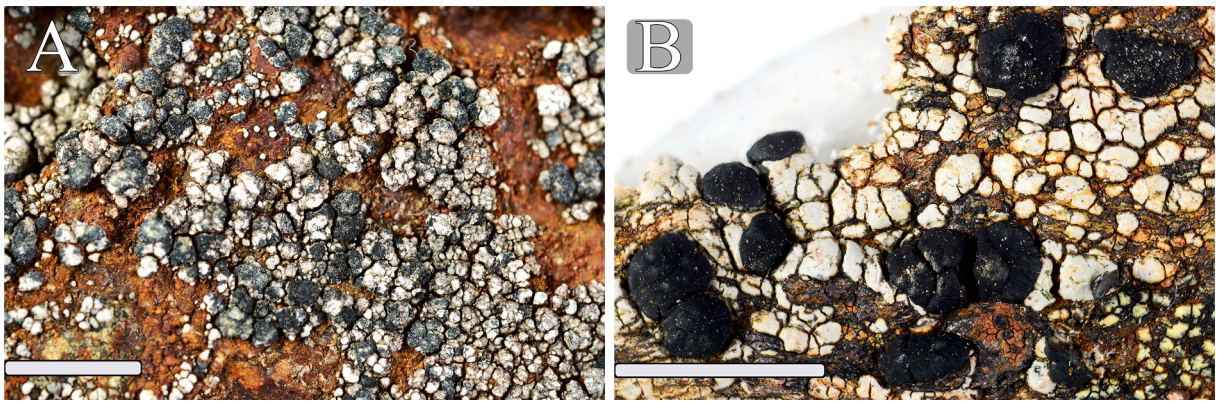

Fig. 8. Morphotypes of *C. cuprea*. **A.** A sorediate specimen of the species (O-L-208192) **B.** One of the two esorediate and fertile specimens (O-L-228131) highlighted in red in Fig. 3 (MEL2021_50_CUP). (For interpretation of the references to color in this figure legend, the reader is referred to the web version of this article.)

The term sibling species may be relevant for clades that are closely related, monophyletic, genetically distinct, and seemingly phenotypically indistinguishable, such as the clades "a" and "b" in *C. aglaea* (Fig. 3A). The phenotypic similarity between sibling species is thought to arise through morphological stasis (Lumbsch and Leavitt, 2011). As described by Struck et al. (2018a), the lack of morphological diversification can be due to low standing genetic variation and/or developmental constraints. The authors also point out that the ecology of taxa showing stasis can have remained constant through time, thereby causing stabilizing selection to retain a shared morphology. Even if two species that are seemingly identical in morphology are genetically distinct, it does not necessarily imply that they are cryptic. As proposed by Struck et al. (2018a), a quantitative assessment of phenotypic similarity should be applied in an evolutionary context.

4.5. Methods and troubleshooting - potential pitfalls of reconstructing evolutionary histories

Given our problems with resolving the interrelationships among the Tephromelataceae genera and subgenera, we dug deeper into the nature of the loci used for phylogenetic inference. Our results show indication of saturation of substitutions for the protein coding MCM7 (Fig. 5). Substitutional saturation is a well-known source of non-phylogenetic signals. Spribille et al. (2011b) published parallel findings for MCM7 in the related genus *Mycoblastus*. Hence, we recommend that careful measures are taken when using this gene (by e.g., translating nucleotides to amino acid prior to phylogenetic analyses), in particular for the Tephromelataceae, as strong non-phylogenetic signals may result in unreliable topologies and support values (cf. Philippe et al., 2011).

The higher terminal resolution of the ITS corresponds to the higher density of relatively short distances compared to MCM7 and TEF1-α (Fig. 5B and S1). The distribution of genetic distances for the three nuclear loci reflects their levels of variability (Fig. 5B). Interspecific variation in regions such as the ITS can be maintained because of a non-selective constraint on non-coding regions (Ganley & Kobayashi, 2007). This is perhaps the most important reason for the elevated level of variability in the ITS, compared to the two other nuclear markers (MCM7 and TEF1-α), which are subjected to purifying selection at their first and second codon positions to maintain protein function. The MCM7 and TEF1-α have lower densities of distances than the ITS in the range 0.05 to 0.10 (Fig. 5B), and they provide lower terminal resolution but slightly more resolved backbones in the gene trees (Fig. S1). In addition, the near absence of distances observed for TEF1-α seems to be connected to the short and poorly supported branches leading up to the subgenus *Calvitimela*, *Severidea* and *Tephromela* (Fig. S1E-F). We detected no differences in saturation plots when excluding the outgroup taxa. This suggests that the main lineages in the Tephromelataceae are quite divergent, also compared to the outgroup.

The major clades in the Tephromelataceae (i.e., genera and subgenera) were topologically congruent and 95 % HPD age estimate intervals were overlapping between the strict and relaxed analyses (Fig. 6; Table S4). However, the strict clock always had consistently older median estimates compared to the relaxed clock (Table S4). Summarizing trees from the posterior of the strict and relaxed analysis yielded different backbone topologies, which may have affected node age estimations because of topological uncertainties. Molecular dating has become increasingly popular and is a valuable technique for understanding at which time scales evolutionary processes occur (e.g., Divakar et al., 2017; Huang et al., 2019; Nelsen et al., 2020). However, the scarce fossil record for lichens (Honegger et al., 2013) is a major obstacle for obtaining accurate estimates of divergence times. The fossil calibration scheme used by Nelsen et al. (2020) is one of the most extensive to date, with thorough justification of the different calibrations used and a broad sampling across the fungal kingdom. Still, there can be severe effects in the estimated node ages from which type of calibrations (e.g., fossils or prior distributions) are used, and how they are set (e.g., fixed ages, or constrained ages; Sauquet, 2013). The taxon sampling can also affect the outcome by introducing larger intervals of node age estimates with smaller sample sizes (Soares & Schrago, 2012).

In general, there are many uncertainties when performing molecular dating analyses, particularly when applying secondary calibrations (see Sauquet, 2013) and the results should be interpreted with caution. Our analysis may have been run by explicitly sampling from the prior, to assess the prior setting effect on the output (see Pardo-De la Hoz et al., 2023). Since we only set out to provide an initial framework for discussing evolutionary histories and to guide in taxonomic conclusions, these options were left out, but should be considered in future studies.

The study by Divakar et al. (2017) is one of the few studies including sequences of *Mycoblastus* and *Tephromela* in a molecular dating framework. We did not set out to discuss the divergence time of these two genera and seeing that the sampling schemes between this study and Divakar et al. (2017) are very different, it is not meaningful to discuss potential discrepancies between age estimates.

5. Conclusion

This study has corroborated an unresolved *Calvitimela* with a substantial increase in molecular data compared to previous studies. In a broad sense, a few but recognizable morphological traits connect the subgenera of *Calvitimela* together. Chemically, species belonging to *Calvitimela* are distinguishable from the other genera in the Tephromelataceae, but not always within the subgenera. To reach any satisfying circumscription of genera in the family, our results strongly suggest that additional molecular data is needed.

The three genetically divergent clades of *C. melaleuca* s. lat. coexist and share similar ecological niches. They have overlapping chemistries

and to some extent morphologies, however spore size and thallus color seem to be diagnostic characters. We suggest that the four genetic lineages in the subgenus *Calvitimela* should be treated as separate taxa. In *Severidea* both morphological and chemical characters are overlapping, but phylogenetic evidence suggest that the clearly divergent clade *C.* sp. also should be recognized as a distinct taxon. The esorediate and fertile morphotype of *C. cuprea* is conspecific with the sorediate morphotype. Lastly, the taxonomic novelties discovered in this study require names, and therefore a proper nomenclatural treatment is under preparation.

In *Calvitimela*, the distinction between cryptic and non-cryptic diversity is not consistently clear-cut, with the varying degrees of character overlap and mismatch to the DNA based phylogeny. This study is only a tiny cut into the evolution and diversity of *Calvitimela* s. lat. However, we did sample the described diversity worldwide, but the uncovering of cryptic diversity in Norway may suggest that a deep well of undiscovered diversity could exist at a global level.

Future work should aim at a more extensive population sampling in subgenus *Calvitimela*, using multiple markers to elucidate species distributions, and population genetic analyses to better understand population structure. If questions about deep phylogenetic relationships in the Tephromelataceae are to be understood, more and new, preferably highly conserved markers, are needed. Whole genome data is likely to reveal interesting results about the ancient evolutionary history of the genus and the family. Lastly, molecular work on the photobiont must be considered when dealing with patterns of cryptic diversity in lichens.

CRediT authorship contribution statement

Markus Osaland Fjelde: Conceptualization, Writing – original draft, Methodology, Formal analysis. **Einar Timdal:** Methodology, Resources, Writing – review & editing, Project administration. **Reidar Haugan:** Methodology, Resources, Writing – review & editing. **Mika Bendiksby:** Methodology, Conceptualization, Resources, Writing – review & editing, Project administration.

Declaration of Competing Interest

The authors declare that they have no known competing financial interests or personal relationships that could have appeared to influence the work reported in this paper.

Acknowledgements

This research was undertaken as part of a master's project at Natural History Museum, University of Oslo, from which all resources used also originate. The authors would like to thank curators at GZU, KGLO, MSC, QFA, UPS and WIS for providing valuable material for this study. More generally, we are grateful to all the collectors of the specimens that we have studied. Siri Rui is thanked for technical support in the fungarium and Lisbeth Thorbek in the NHM molecular laboratory. Thanks also to Klara Scharnagl and Vladimir Gusarov for fruitful feedback as sensors during my master's exam.

Appendix A. Supplementary material

Supplementary data to this article can be found online at https://doi.org/10.1016/j.ympev.2023.107944.

References

Adobe Inc., 2020. Adobe InDesign. Retrieved from https://adobe.com/products/indesign.

Alda, F., Tagliacollo, V.A., Bernt, M.J., Waltz, B.T., Ludt, W.B., Faircloth, B.C., et al., 2019. Resolving deep nodes in an ancient radiation of neotropical fishes in the presence of conflicting signals from incomplete lineage sorting. Syst. Biol. 68 (4), 573–593. https://doi.org/10.1093/sysbio/syy085.

Arnold, A.E., Miadlikowska, J., Higgins, K.L., Sarvate, S.D., Gugger, P., Way, A., et al., 2009. A phylogenetic estimation of trophic transition networks for ascomycetous fungi: are lichens cradles of symbiotrophic fungal diversification? Syst. Biol. 58 (3), 283–297. https://doi.org/10.1093/sysbio/syp001.

Asplund, J., Siegenthaler, A., Gauslaa, Y., 2017. Simulated global warming increases usnic acid but reduces perlatolic acid in the mat-forming terricolous lichen Cladonia stellaris. Lichenologist 49 (3), 269–274. https://doi:10.1017/S0024282917000159.

Bendiksby, M., Timdal, E., 2013. Molecular phylogenetics and taxonomy of Hypocenomyce sensu lato (Ascomycota: Lecanoromycetes): extreme polyphyly and morphological/ecological convergence. Taxon 62, 940–956. https://doi.org/10.12705/625.18.

Bendiksby, M., Haugan, R., Spribille, T., Timdal, E., 2015. Molecular Phylogenetics and Taxonomy of the Calvitimela aglaea complex (Tephromelataceae, Lecanorales). Mycologia 107 (1), 1172–1183. https://doi.org/10.3852/14-062.

Bouckaert, R., Vaughan, T.G., Barido-Sottani, J., Duchêne, S., Fourment, M., Gavryushkina, A., Heled, J., Jones, G., Kühnert, D., De Maio, N., 2019. Beast 2.5: An Advanced Software Platform for Bayesian Evolutionary Analysis. PLoS Comput. Biol. 15 (4), e1006650.

Cardinale, M., Puglia, A.M., Grube, M., 2006. Molecular analysis of lichen-associated bacterial communities. FEMS Microbiol. Ecol. 57 (3), 484–495. https://doi.org/10.1111/j.1574-6941.2006.00133.x.

Castresana, J., 2000. Selection of conserved blocks from multiple alignments for their use in phylogenetic analysis. Mol. Biol. Evol. 17 (4), 540–552. https://doi.org/10.1093/oxfordjournals.molbev.a026334.

Crespo, A., Lumbsch, H.T., 2010. Cryptic Species in Lichen-Forming Fungi. IMA fungus 1 (2), 167. https://doi.org/10.5598/imafungus.2010.01.02.09.

Culberson, C.F., 1972. Improved Conditions and New Data for Identification of Lichen Products by Standardized Thin Layer Chromatographic Method. J. Chromatogr. A 72 (1), 113–125. https://doi.org/10.1016/0021-9673(72)80013-X.

Culberson, W.L., 1986. Chemistry and sibling speciation in the lichen-forming fungi: ecological and biological considerations. Bryologist 123–131. https://doi/10.2307/3242752.

Culberson, C.F., Culberson, W.L., 1976. Chemosyndromic variation in lichens. Syst. Bot. 325–339 https://doi.org/10.2307/2418700.

Culberson, C.F., Johnson, A., 1982. Substitution of Methyl Tert. - Butyl Ether for Diethyl Ether in the Standardized Thin-Layer Chromatographic Method for Lichen Products. J. Chromatogr. A 238 (2), 483–547. https://doi.org/10.1016/S0021-9673(00)81336-9.

Culberson, C.F., Kristinsson, H.D., 1970. A Standardized Method for the Identification of Lichen Products. J. Chromatogr. A 46, 85–93. https://doi.org/10.1016/S0021-9673(00)83967-9.

Delsuc, F., Brinkmann, H., Philippe, H., 2005. Phylogenomics and the reconstruction of the tree of life. Nat. Rev. Genet. 6 (5), 361–375. https://doi.org/10.1038/nrg1603.

Divakar, P.K., Crespo, A., Kraichak, E., Leavitt, S.D., Singh, G., Schmitt, I., Lumbsch, H. T., 2017. Using a temporal phylogenetic method to harmonize family-and genus-level classification in the largest clade of lichen-forming fungi. Fungal Divers. 84 (1), 101–117. https://doi.org/10.1007/s13225-017-0379-z.

Edgar, R.C., 2004. Muscle: Multiple Sequence Alignment with High Accuracy and High Throughput. Nucleic Acids Res. 32 (5), 1792–2177. https://doi.org/10.1093/nar/gkh340.

Ertz, D., Guzow-Krzemińska, B., Thor, G., Łubek, A., Kukwa, M., 2018. Photobiont switching causes changes in the reproduction strategy and phenotypic dimorphism in the Arthoniomycetes. Sci. Rep. 8 (1), 1–14. https://doi.org/10.1038/s41598-018-23219-3.

Färber, L., Solhaug, K.A., Esseen, P.A., Bilger, W., Gauslaa, Y., 2014. Sunscreening fungal pigments influence the vertical gradient of pendulous lichens in boreal forest canopies. Ecology 95 (6), 1464–1471. https://doi.org/10.1890/13-2319.1.

Frolov, I., Vondrák, J., Fernández-Mendoza, F., Wilk, K., Khodosovtsev, A., & Halıcı, M. G. 2016. Three new, seemingly-cryptic species in the lichen genus *Caloplaca* (Teloschistaceae) distinguished in two-phase phenotype evaluation. In *Annales Botanici Fennici* (Vol. 53. No. 3–4, p. 243-262). Finnish Zoological and Botanical Publishing Board. https://doi.org/10.5735/085.053.0413.

Ganley, A.R., Kobayashi, T., 2007. Highly efficient concerted evolution in the ribosomal DNA repeats: total rDNA repeat variation revealed by whole-genome shotgun sequence data. Genome Res. 17 (2), 184–191. https://doi:10.1101/gr.5457707.

Garrido-Benavent, I., Pérez-Ortega, S., de Los Ríos, A., Mayrhofer, H., Fernández-Mendoza, F., 2021. Neogene speciation and Pleistocene expansion of the genus Pseudephebe (Parmeliaceae, lichenized fungi) involving multiple colonizations of Antarctica. Mol. Phylogenet. Evol. 155, 107020 https://doi.org/10.1016/j.ympev.2020.107020.

Gaya, E., Fernández-Brime, S., Vargas, R., Lachlan, R. F., Gueidan, C., Ramírez-Mejía, M., & Lutzoni, F. 2015. The adaptive radiation of lichen-forming Teloschistaceae is associated with sunscreening pigments and a bark-to-rock substrate shift. Proceedings of the National Academy of Sciences **112**(37): 11600-11605. https://doi.org/10.1073/pnas.1507072112.

Guindon, S., Dufayard, J.F., Lefort, V., Anisimova, M., Hordijk, W., Gascuel, O., 2010. New algorithms and methods to estimate maximum-likelihood phylogenies: assessing the performance of PhyML 3.0. Syst. Biol. 59 (3), 307–321. https://doi.org/10.1093/sysbio/syq010.

Haugan, R., Timdal, E., 1994. *Tephromela perlata* and *T. talayana*, with notes on the *T. aglaea*- complex. Graphis Scripta 6 (1), 17–26.

Hertel, H., Rambold, G., 1985. Lecidea Sect. Armeniacae: Lecideoide Arten Der Flechtengattungen Lecanora Und Tephromela (Lecanorales). Pflanzengeschichte und Pflanzengeographie.

Hodkinson, B.P., Lutzoni, F., 2009. A microbiotic survey of lichen-associated bacteria reveals a new lineage from the Rhizobiales. Symbiosis 49, 163–180. https://doi.org/10.1007/s13199-009-0049-3.
Honegger, R., Edwards, D., Axe, L., 2013. The earliest records of internally stratified cyanobacterial and algal lichens from the Lower Devonian of the Welsh Borderland. New Phytol. 197 (1), 264–275. https://doi.org/10.1111/nph.12009.
Huang, J.P., Kraichak, E., Leavitt, S.D., Nelsen, M.P., Lumbsch, H.T., 2019. Accelerated diversifications in three diverse families of morphologically complex lichen-forming fungi link to major historical events. Sci. Rep. 9 (1), 1–10. https://doi.org/10.1038/s41598-019-44881-1.
Kantvilas, G., 2009. The genus Mycoblastus in the cool temperate Southern Hemisphere, with special reference to Tasmania. Lichenologist 41(2), 151–178. https://doi:10.1017/S0024282909008238.
Kelly, L.J., Hollingsworth, P.M., Coppins, B.J., Ellis, C.J., Harrold, P., Tosh, J., Yahr, R., 2011. DNA barcoding of lichenized fungi demonstrates high identification success in a floristic context. New Phytol. 191 (1), 288–300. https://doi.org/10.1111/j.1469-8137.2011.03677.x.
Keuler, R., Jensen, J., Barcena-Peña, A., Grewe, F., Lumbsch, H.T., Huang, J.P., Leavitt, S.D., 2022. Interpreting phylogenetic conflict: Hybridization in the most speciose genus of lichen-forming fungi. Mol. Phylogenet. Evol. 107543 https://doi.org/10.1016/j.ympev.2022.107543.
Kimura, M., 1980. A simple method for estimating evolutionary rates of base substitutions through comparative studies of nucleotide sequences. J. Mol. Evol. 16 (2), 111–120. https://doi.org/10.1007/BF01731581.
Kistenich, S., Rikkinen, J.K., Thüs, H., Vairappan, C.S., Wolseley, P.A., Timdal, E., 2018. Three new species of Krogia (Ramalinaceae, lichenised Ascomycota) from the Paleotropics. MycoKeys 40, 69. https://doi.org/10.3897/mycokeys.40.26025.
Kozlov, A.M., Darriba, D., Flouri, T., Morel, B., Stamatakis, A., 2019. RAxML-NG: a fast, scalable and user-friendly tool for maximum likelihood phylogenetic inference. Bioinformatics 35 (21), 4453–4455. https://doi.org/10.1093/bioinformatics/btz305.
LaGreca, S., Lumbsch, H.T., Kukwa, M., Wei, X., Han, J.E., Moon, K.H., et al., 2020. A molecular phylogenetic evaluation of the *Ramalina siliquosa* complex, with notes on species circumscription and relationships within *Ramalina*. Lichenologist 52 (3), 197–211. https://doi:10.1017/S0024282920000110.
Lanfear, R., Calcott, B., Ho, S.Y., Guindon, S., 2012. PartitionFinder: combined selection of partitioning schemes and substitution models for phylogenetic analyses. Mol. Biol. Evol. 29 (6), 1695–1701. https://doi.org/10.1093/molbev/mss020.
Lanfear, R., Frandsen, P.B., Wright, A.M., Senfeld, T., Calcott, B., 2016. PartitionFinder 2: new methods for selecting partitioned models of evolution for molecular and morphological phylogenetic analyses. Mol. Biol. Evol. 34 (3), 772–773. https://doi.org/10.1093/molbev/msw260.
Leavitt, S.D., Fankhauser, J.D., Leavitt, D.H., Porter, L.D., Johnson, L.A., Clair, L.L.S., 2011. Complex patterns of speciation in cosmopolitan "rock posy" lichens–Discovering and delimiting cryptic fungal species in the lichen-forming Rhizoplaca melanophthalma species-complex (Lecanoraceae, Ascomycota). Mol. Phylogenet. Evol. 59 (3), 587–602. https://doi.org/10.1016/j.ympev.2011.03.020.
Leavitt, S.D., Kraichak, E., Vondrak, J., Nelsen, M.P., Sohrabi, M., Perez-Ortega, S., et al., 2016. Cryptic diversity and symbiont interactions in rock-posy lichens. Mol. Phylogenet. Evol. 99, 261–274. https://doi.org/10.1016/j.ympev.2016.03.030.
Lemmon, E.M., Lemmon, A.R., 2013. High-throughput genomic data in systematics and phylogenetics. Annu. Rev. Ecol. Evol. Syst. 44, 99–121. https://doi.org/10.1146/annurev-ecolsys-110512-135822.
Lendemer, J.C., Harris, R.C., 2016. Studies in Lichens and Lichenicolous Fungi–No. 20: Further notes on species from the eastern North America. Opuscula Philolichenum 15, 105–131.
Lücking, R., Hodkinson, B.P., Leavitt, S.D., 2017. The 2016 classification of lichenized fungi in the Ascomycota and Basidiomycota-Approaching one thousand genera. Bryologist 119 (4), 361–416.
Lücking, R., Aime, M.C., Robbertse, B., Miller, A.N., Ariyawansa, H.A., Aoki, T., et al., 2020. Unambiguous identification of fungi: where do we stand and how accurate and precise is fungal DNA barcoding? IMA fungus 11 (1), 1–32.
Lumbsch, H.T., Ahti, T., Altermann, S., De Paz, G.A., Aptroot, A., Arup, U., et al., 2011. One hundred new species of lichenized fungi: a signature of undiscovered global diversity. Phytotaxa 18 (1), 1–127. https://doi.org/10.11646/phytotaxa.18.1.1.
Lumbsch, H.T., Leavitt, S.D., 2011. Goodbye morphology? A paradigm shift in the delimitation of species in lichenized fungi. Fungal Divers. 50 (1), 59–72. https://doi.org/10.1007/s13225-011-0123-z.
Lutzoni, F., Kauff, F., Cox, J.C., McLaughlin, D., Celio, G., Dentinger, B., Padamsee, M., Hibbett, D., James, T.Y., Baloch, E., Grube, M., Reeb, V., Hofstetter, V., Schoch, C., Arnold, A.E., Miadlikowska, J., Spatafora, J., Johnson, D., Hambleton, S., Crockett, M., Shoemaker, R., Sung, G.-H., Lücking, R., Lumbsch, T., O'Donnell, K., Binder, M., Diederich, P., Ertz, D., Gueidan, C., Hansen, K., Harris, R.C., Hosaka, K., Lim, Y.-W., Matheny, B., Nishida, H., Pfister, D., Rogers, J., Rossman, A., Schmitt, I., Sipman, H., Stone, J., Sugiyama, J., Yahr, R., Vilgalys, R., 2004. Assembling the fungal tree of life: Progress, classification, and evolution of subcellular traits. Am. J. Bot. 91, 1446–1480. https://doi.org/10.3732/ajb.91.10.1446.
Mann, D. G., & Evans, K. M. 2008. The species concept and cryptic diversity. In *Proceedings of the 12th International Conference on Harmful Algae* (p. 262-268). Copenhagen: International Society for the Study of Harmful Algae and Intergovernmental Oceanographic Commission of UNESCO.
Marthinsen, G., Rui, S., Timdal, E., 2019. OLICH: A reference library of DNA barcodes for Nordic lichens. Biodivers. Data J. 7, e36252.
Mattsson, J.E., Lumbsch, H.T., 1989. The use of the species pair concept in lichen taxonomy. Taxon 38 (2), 238–241. https://doi.org/10.2307/1220840.
McCune, B. 2017. Microlichens of the Pacific Northwest. Volume 2: Key to the species. Corvallis. Wild Blueberry Media. ISBN: 9-780998-710808.
Menlove, J.E., 1974. Thin-Layer Chromatography for the Identification of Lichen Substances. British Lichen Society Bulletin 34, 3–5.
Muggia, L., Grube, M., Tretiach, M., 2008. Genetic diversity and photobiont associations in selected taxa of the Tephromela atra group (Lecanorales, lichenised Ascomycota). Mycol. Prog. 7 (3), 147–160. https://doi.org/10.1007/s11557-008-0560-6.
Næsborg, R.R., Ekman, S., Tibell, L., 2007. Molecular phylogeny of the genus Lecania (Ramalinaceae, lichenized Ascomycota). Mycol. Res. 111 (5), 581–591. https://doi.org/10.1016/j.mycres.2007.03.001.
Nash, T. H. 2008. *Lichen biology* (2nd ed., pp. IX, 486). Cambridge University Press.
Nelsen, M.P., Lücking, R., Boyce, C.K., Lumbsch, H.T., Ree, R.H., 2020. No support for the emergence of lichens prior to the evolution of vascular plants. Geobiology 18 (1), 3–13. https://doi.org/10.1111/gbi.12369.
Paradis, E., 2010. pegas: an R package for population genetics with an integrated-modular approach. Bioinformatics 26 (3), 419–420. https://doi.org/10.1093/bioinformatics/btp696.
Paradis, E., Schliep, K., 2019. ape 5.0: an environment for modern phylogenetics and evolutionary analyses in R. Bioinformatics 35 (3), 526–528. https://doi.org/10.1093/bioinformatics/bty633.
Pardo-De la Hoz, C.J., Magain, N., Piatkowski, B., Cornet, L., Dal Forno, M., Carbone, I., Miadlikowska, J., Lutzoni, F., 2023. Ancient rapid radiation explains most conflicts among gene trees and well-supported phylogenomic trees of Nostocalean cyanobacteria. Syst. Biol. 72, 694–712. https://doi.org/10.1093/sysbio/syad008.
Philippe, H., Brinkmann, H., Lavrov, D.V., Littlewood, D.T.J., Manuel, M., Wörheide, G., Baurain, D., 2011. Resolving difficult phylogenetic questions: why more sequences are not enough. PLoS Biol. 9 (3), e1000602.
Pizarro, D., Divakar, P. K., Grewe, F., Leavitt, S. D., Huang, J. P., Dal Grande, F., et al., 2018. Phylogenomic analysis of 2556 single-copy protein-coding genes resolves most evolutionary relationships for the major clades in the most diverse group of lichen-forming fungi. *Fungal diversity* **92**(1): 31-41. https://doi.org/10.1007/s13225-018-0407-7.
Poelt, J., 1970. Das Konzept der Artenpaare bei den Flechten. Deutsche Botanische Gesellschaft, neue Folge 4, 187–198.
Purvis, & British Lichen Society. 1992. The Lichen flora of Great Britain and Ireland (p. 704). Natural History Museum Publications in association with The British Lichen Society. ISBN: 0565011634.
R Core Team, 2020. R: A language and environment for statistical computing. R Foundation for Statistical Computing, Vienna, Austria https://www.R-project.org/.
Rambaut, A., Drummond, A. J., Xie, D., Baele, G., & Suchard, M. A. 2018. Posterior Summarization in Bayesian Phylogenetics Using Tracer 1.7. *Systematic Biology* **67**(5): 901-04. https://doi.org/10.1093/sysbio/syy032.
Ronquist, F., Teslenko, M., Van Der Mark, P., Ayres, D. L., Darling, A., Höhna, S., et al., 2012. MrBayes 3.2: efficient Bayesian phylogenetic inference and model choice across a large model space. *Systematic biology* **61**(3): 539-542. https://doi.org/10.1093/sysbio/sys029.
Schneider, K., Resl, P., Westberg, M., Spribille, T., 2015. A new, highly effective primer pair to exclude algae when amplifying nuclear large ribosomal subunit (LSU) DNA from lichens. Lichenologist 47 (4), 269. https://doi:10.1017/S002428291500016X.
Schneider, K., Resl, P., Spribille, T., 2016. Escape from the cryptic species trap: lichen evolution on both sides of a cyanobacterial acquisition event. Mol. Ecol. 25 (14), 3453–3468. https://doi.org/10.1111/mec.13636.
Schwendener, S., 1869. Die algentypen der Flechtengonidien. C. Schultze.
Singh, G., Dal Grande, F., Divakar, P.K., Otte, J., Leavitt, S.D., Szczepanska, K., et al., 2015a. Coalescent-based species delimitation approach uncovers high cryptic diversity in the cosmopolitan lichen-forming fungal genus Protoparmelia (Lecanorales, Ascomycota). PLoS One 10 (5), e0124625.
Singh, G., Dal Grande, F., Werth, S., Scheidegger, C., 2015b. Long-term consequences of disturbances on reproductive strategies of the rare epiphytic lichen Lobaria pulmonaria: clonality a gift and a curse. FEMS Microbiol. Ecol. 91 (1), 1–11. https://doi:10.1093/femsec/fiu009.
Soares, A.E., Schrago, C.G., 2012. The influence of taxon sampling and tree shape on molecular dating: an empirical example from Mammalian mitochondrial genomes. Bioinf. Biol. Insights 6, BBI-S9677. https://doi.org/10.4137/BBI.S9677.
Spribille, T., 2018. Relative symbiont input and the lichen symbiotic outcome. Curr. Opin. Plant Biol. 44, 57–63. https://doi.org/10.1016/j.pbi.2018.02.007.
Spribille, T., Tuovinen, V., Resl, P., Vanderpool, D., Wolinski, H., Aime, M. C., et al., 2016. Basidiomycete yeasts in the cortex of ascomycete macrolichens. *Science* **353** (6298): 488-492. 10.1126/science.aaf8287.
Spribille, T., Goffinet, B., Barbara, K., Muggia, L., Obermayer, W., Mayrhofer, H., 2011a. Molecular Support for the Recognition of the Mycoblastus fucatus Group as the New Genus Violella (Tephromelataceae, Lecanorales). Lichenologist 43 (5), 445–466. https://doi.org/10.1017/S0024282911000478.
Spribille, T., Klug, B., Mayrhofer, H., 2011b. A phylogenetic analysis of the boreal lichen Mycoblastus sanguinarius (Mycoblastaceae, lichenized Ascomycota) reveals cryptic clades correlated with fatty acid profiles. Mol. Phylogenet. Evol. 59 (3), 603–614. https://doi.org/10.1016/j.ympev.2011.03.021.
Steinová, J., Holien, H., Košuthová, A., Škaloud, P., 2022. An Exception to the Rule? Could Photobiont Identity Be a Better Predictor of Lichen Phenotype than Mycobiont Identity? Journal of Fungi 8 (3), 275. https://doi.org/10.3390/jof8030275.
Stenroos, S., Velmala, S., Pykälä, J., Ahti, T., 2016. Lichens of Finland. Botanical Museum, Finnish Museum of Natural History.
Struck, T.H., Feder, J.L., Bendiksby, M., Birkeland, S., Cerca, J., Gusarov, V.I., et al., 2018a. Finding evolutionary processes hidden in cryptic species. Trends Ecol. Evol. 33 (3), 153–163. https://doi.org/10.1016/j.tree.2017.11.007.

Talavera, G., Castresana, J., 2007. Improvement of phylogenies after removing divergent and ambiguously aligned blocks from protein sequence alignments. Syst. Biol. 56 (4), 564–577. https://doi.org/10.1080/10635150701472164.
Taylor, J.W., Jacobson, D.J., Kroken, S., Kasuga, T., Geiser, D.M., Hibbett, D.S., Fisher, M.C., 2000. Phylogenetic species recognition and species concepts in fungi. Fungal Genet. Biol. 31 (1), 21–32. https://doi:10.1006/fgbi.2000.1228.
White, T.J., Bruns, T., Lee, S.J.W.T., Taylor, J., 1990. Amplification and direct sequencing of fungal ribosomal RNA genes for phylogenetics. In: Innis, M.A., Gelfand, D.H., Sninsky, J.J., White, T.J. (Eds.), PCR Protocols: a Guide to Methods and Applications. Academic Press Inc, New York, pp. 315–322.
Wickham, H., 2016. ggplot2: Elegant Graphics for Data Analysis. Springer-Verlag, New York https://ggplot2.tidyverse.org.
Widhelm, T.J., Grewe, F., Huang, J.P., Mercado-Díaz, J.A., Goffinet, B., Lücking, R., et al., 2019. Multiple historical processes obscure phylogenetic relationships in a taxonomically difficult group (Lobariaceae, Ascomycota). Sci. Rep. 9 (1), 1–16. https://doi.org/10.1038/s41598-019-45455-x.
Zhang, Y., Clancy, J., Jensen, J., McMullin, R.T., Wang, L., Leavitt, S.D., 2022. Providing Scale to a Known Taxonomic Unknown—At Least a 70-Fold Increase in Species Diversity in a Cosmopolitan Nominal Taxon of Lichen-Forming Fungi. Journal of Fungi 8 (5), 490. https://doi.org/10.3390/jof8050490.
Zoller, S., Scheidegger, C., Sperisen, C., 1999. PCR primers for the amplification of mitochondrial small subunit ribosomal DNA of lichen-forming ascomycetes. Lichenologist 31 (5), 511–516. https://doi.org/10.1006/lich.1999.0220.

Further reading

Alfaro, M.E., Zoller, S., Lutzoni, F., 2003. Bayes or bootstrap? A simulation study comparing the performance of Bayesian Markov chain Monte Carlo sampling and bootstrapping in assessing phylogenetic confidence. Mol. Biol. Evol. 20, 255–266. https://doi.org/10.1093/molbev/msg028.
Anderson, J.B., Kohn, L.M., 2007. Dikaryons, diploids, and evolution. In: Sex in Fungi: Molecular Determination and Evolutionary Implications. American Society of Microbiology Press, USA, pp. 333–348.
Andreev, M.P., 2004. New taxonomic combinations for lecidioid lichens. Novosti sistematiki nizshikh rasteniy 37, 188–191.
Fryday, A.M., 2011. New Species and Combinations in *Calvitimela* and *Tephromela* from the Southern Subpolar Region. Lichenologist 43 (3), 225. https://doi:10.1017/S0024282911000065.
Hafellner, J., Türk, R., 2001. Die Lichenisierten Pilze Österreichs: Eine Checkliste Der Bisher Nachgewiesenen Arten Mit Verbreitungsangaben. Biologiezentrum d. Oberösterr, Landesmuseums.
Heethoff, M. 2018. Cryptic species–conceptual or terminological chaos? A response to Struck et al. Trends in Ecology & Evolution 33(5): 310. https://doi.org/10.1016/j.tree.2018.02.006.
Larsson, A., 2014. Aliview: A Fast and Lightweight Alignment Viewer and Editor for Large Datasets. Bioinformatics 30 (22), 3276–3328. https://doi.org/10.1093/bioinformatics/btu531.
Magnusson, A.H., 1931. Studien ÜBer Einige Arten Der *Lecidea armeniaca*- Und *elata*-Gruppe. Acta Horti Gothoburg 6, 93–144.
Rambaut, A. 2012. Figtree v. 1.4.4 Retrieved from https://github.com/rambaut/figtree.
Struck, T.H., Feder, J.L., Bendiksby, M., Birkeland, S., Cerca, J., Gusarov, V.I., et al., 2018b. Cryptic species–more than terminological chaos: a reply to Heethoff. Trends Ecol. Evol. 33 (5), 310–312. https://doi.org/10.1016/j.tree.2018.02.008.